

Monotone-Value Neural Networks: Exploiting Preference Monotonicity in Combinatorial Assignment

Jakob Weissteiner^{1*} Jakob Heiss^{2*} Julien Siems^{1*} Sven Seuken¹

¹UNIVERSITY OF ZURICH
Department of Informatics

²ETH ZURICH
Department of Mathematics

weissteiner@ifi.uzh.ch, jakob.heiss@math.ethz.ch, siems@ifi.uzh.ch, seuken@ifi.uzh.ch

Abstract

Many important resource allocation problems involve the *combinatorial assignment* of items (e.g., combinatorial auctions, combinatorial exchanges, and combinatorial course allocation). Because the bundle space grows exponentially in the number of items, preference elicitation is a key challenge in these domains, in particular because agents may view items as substitutes or complements. Recently, researchers have proposed machine learning (ML)-based mechanisms that outperform traditional mechanisms while reducing preference elicitation costs for agents. However, one major shortcoming of the ML algorithms that were used is that they ignore important prior knowledge about agents' preferences. To address this, we introduce *monotone-value neural networks* (MVNNs), which are carefully designed to capture combinatorial valuations, while enforcing *monotonicity* (i.e., adding an item to a bundle weakly increases its value) and *normality* (i.e., the empty bundle has zero value). On a technical level, we make two main contributions. First, we prove that our MVNNs are universal in the class of monotone and normalized value functions; second, we provide a mixed-integer program (MIP) formulation to make solving MVNN-based winner determination problems practically feasible. We evaluate our MVNNs experimentally in spectrum auction domains. Our results show that MVNNs improve the prediction performance when learning agents' value functions, they improve the allocative efficiency of the auction, and they also reduce the run-time of the winner determination problem.

1 Introduction

Many important economic problems involve the *combinatorial assignment* of multiple indivisible items to multiple agents. In domains *with money*, prominent examples include *combinatorial auctions* (CAs) and *combinatorial exchanges* (CEs). In CAs, heterogeneous items are allocated amongst a set of bidders, e.g. for the sale of spectrum licenses (Cramton 2013). In CEs, a set of items is allocated between multiple agents who can be sellers *and* buyers at the same time, e.g. for the reallocation of catch shares (Bichler, Fux, and Goeree 2019). In domains *without money*, a popular example is *combinatorial course allocation*, where course seats are allocated to students in large business schools (Budish 2011).

*These authors contributed equally.

What all of these domains have in common is that the agents can report their values on *bundles* of items rather than only on individual items. This allows them to express more complex preferences, i.e., their value for a bundle is not just the sum of each individual item's value, but it can be more (*complementarity*) or less (*substitutability*). However, since the bundle space grows exponentially in the number of items, agents cannot report values for all bundles in settings with more than a modest number of items. Thus, parsimonious *preference elicitation* is key for the design of practical combinatorial assignment mechanisms.

In this paper, we present a new machine learning approach that exploits prior (structural) knowledge about agents' preferences and can be integrated well into iterative market mechanisms. Our contribution applies to any combinatorial assignment problem. However, we present our algorithms in the context of a CA specifically, to simplify the notation and because there exist well-studied preference generators for CAs that we can use for our experimental evaluation.

1.1 Iterative Combinatorial Auctions

For CAs with general valuations, Nisan and Segal (2006) have shown that exponential communication in the number of items is needed in the worst case to find an optimal allocation of items to bidders, i.e., to ensure full efficiency. Thus, for general valuations, practical CAs cannot provide efficiency guarantees in large domains. In practice, *iterative combinatorial auctions* (ICAs) are employed, where the auctioneer interacts with bidders over multiple rounds, eliciting a *limited* amount of information, aiming to find a highly efficient allocation. ICAs are widely used; e.g., for the sale of licenses to build offshore wind farms (Ausubel and Cramton 2011). The provision of spectrum licenses via the *combinatorial clock auction* (CCA) (Ausubel, Cramton, and Milgrom 2006) has generated more than \$20 billion in total revenue (Ausubel and Baranov 2017). Therefore, increasing the efficiency of such real-world ICAs by only 1% point translates into monetary gains of hundreds of millions of dollars.

1.2 ML-based Auction Design

In recent years, researchers have successfully integrated machine learning (ML) algorithms into the design of CAs to improve their performance. Early works by Blum et al.

(2004) and Lahaie and Parkes (2004) laid the foundation by establishing a connection between computational learning theory and preference elicitation in CAs. Dütting et al. (2019) and Rahme et al. (2020) used neural networks (NNs) to learn entire auction mechanisms (i.e., an allocation and payment rule) from data, following the automated mechanism design paradigm. Brero, Lahaie, and Seuken (2019) studied a Bayesian ICA using probabilistic price updates to achieve faster convergence to an efficient allocation.

Most related to this paper is the work by Brero, Lubin, and Seuken (2018; 2021), who developed a value-query-based ML-powered ICA that achieves even higher efficiency than the widely used CCA. A key contribution in that work was showing how the ML-based winner determination problem (WDP) can be formulated as a mixed integer program (MIP), such that the WDP can be solved sufficiently quickly in practice. In follow-up work, Weissteiner and Seuken (2020) extended their work by integrating Neural Networks (NN) in their mechanisms and could further increase the efficiency. Finally, Weissteiner et al. (2020) used Fourier transforms to exploit different notions of sparsity of value functions to enhance preference elicitation. However, despite these advances, it remains a challenging problem to find the efficient allocation while keeping the elicitation cost for bidders low. Even state-of-the-art approaches suffer from significant efficiency losses, highlighting the need for better preference elicitation algorithms.

We show in this paper that these limitations can be partially explained due to the usage of poor, non-informative ML-algorithms, which either do not include important prior domain knowledge or make too restrictive assumptions about the bidders' value functions. Brero, Lubin, and Seuken (2018; 2021) used SVRs with quadratic kernels (which can only learn up to two way interactions between items) and they also did not account for an important monotonicity property of bidders' value functions in the ML-algorithm. While the fully-connected feed-forward NNs used by Weissteiner and Seuken (2020) are a more expressive ML algorithm, they also do not account for this monotonicity property. In particular when operating with only a small number of data points per bidder (which is the standard in market mechanisms, because preference elicitation is costly), this can cause significant efficiency losses.

Over the last decade, major successes in the ML-community were made by specialized NN architectures (e.g. CNNs) that incorporate domain-specific prior knowledge to improve generalization (Bronstein et al. 2017). In this paper, we follow the same paradigm by incorporating prior knowledge about monotone preferences into a NN architecture to improve generalization, which is key for a well-functioning preference elicitation algorithm. Several other approaches for incorporating monotonicity into NNs have been proposed in the literature (Sill 1998; You et al. 2017; Wehenkel and Louppe 2019; Liu et al. 2020). However, for these architectures, it is not known how the resulting NN-based WDP could be solved quickly. In contrast, our architecture is particularly well suited for combinatorial assignment problems, because the NN-based WDP can be formulated as a succinct MIP, enabling us to quickly solve the WDP.

1.3 Our Contribution

We propose a new ML algorithm we call *monotone-value neural network (MVNN)*, which is carefully designed to model *monotone* combinatorial value functions. Specifically, we make the following contributions:

1. We introduce MVNNs, a new class of NNs with a carefully designed activation function (bReLU) and enforced constraints on the parameters such that they are normalized and fulfill a monotonicity property (Section 3). These MVNNs are specifically suited to model monotone (combinatorial) value functions in economic settings.
2. On a technical level, we provide in Section 3.1 the following two theorems: First, we prove that MVNNs are universal in the class of monotone and normalized combinatorial value functions, i.e., one can represent *any* value function with arbitrarily complex substitutabilities and complementarities exactly as an MVNN. Second, we show how to formulate the MVNN-based winner determination problem (WDP) as a MIP, which is key to efficiently calculate optimal allocations.
3. We experimentally evaluate the learning performance of MVNNs vs. NNs in four different spectrum CA domains and show that MVNNs can significantly better model bidders' combinatorial value functions (Section 4).
4. Finally, we experimentally investigate the performance of MVNNs vs. plain NNs when integrated into an existing ML-based ICA (MLCA) and show that MVNNs lead to substantially smaller efficiency losses (Section 5).

2 Preliminaries

In this section, we present our formal model and review the ML-based ICA by Brero, Lubin, and Seuken (2021).

2.1 Formal Model for ICAs

We consider a CA with n bidders and m indivisible items. Let $N = \{1, \dots, n\}$ and $M = \{1, \dots, m\}$ denote the set of bidders and items, respectively. We denote with $x \in \mathcal{X} = \{0, 1\}^m$ a bundle of items represented as an indicator vector, where $x_j = 1$ iff item $j \in M$ is contained in x . Bidders' true preferences over bundles are represented by their (private) value functions $v_i : \mathcal{X} \rightarrow \mathbb{R}_+$, $i \in N$, i.e., $v_i(x)$ represents bidder i 's true value for bundle x .

By $a = (a_1, \dots, a_n) \in \mathcal{X}^n$ we denote an allocation of bundles to bidders, where a_i is the bundle bidder i obtains. We denote the set of *feasible* allocations by $\mathcal{F} = \{a \in \mathcal{X}^n : \sum_{i \in N} a_{ij} \leq 1, \forall j \in M\}$. The (true) *social welfare* of an allocation a is defined as $V(a) = \sum_{i \in N} v_i(a_i)$. We let $a^* \in \arg\max_{a \in \mathcal{F}} V(a)$ be a social-welfare maximizing, i.e., *efficient*, allocation. The *efficiency* of any allocation $a \in \mathcal{F}$ is $V(a)/V(a^*)$.

An ICA *mechanism* defines how the bidders interact with the auctioneer and how the final allocation and payments are determined. We denote a bidder's (possibly untruthful) reported value function by $\hat{v}_i : \mathcal{X} \rightarrow \mathbb{R}_+$. In this paper, we consider ICAs that ask bidders to iteratively report their values $\hat{v}_i(x)$ for particular bundles x selected by the mechanism. A set of $L \in \mathbb{N}$ reported bundle-value pairs of bidder i is denoted as $R_i = \{(x^{(l)}, \hat{v}_i(x^{(l)}))\}_{l=1}^L, x^{(l)} \in \mathcal{X}$.

Let $R = (R_1, \dots, R_n)$ denote the tuple of reported bundle-value pairs obtained from all bidders and $R_{-i} = (R_1, \dots, R_{i-1}, R_{i+1}, \dots, R_n)$. We define the *reported social welfare* of an allocation a given R as $\hat{V}(a|R) = \sum_{i \in N: (a_i, \hat{v}_i(a_i)) \in R_i} \hat{v}_i(a_i)$, where $(a_i, \hat{v}_i(a_i)) \in R_i$ ensures that only values for reported bundles contribute. Finally, the optimal allocation $a_R^* \in \mathcal{F}$ given the reports R is defined as

$$a_R^* \in \operatorname{argmax}_{a \in \mathcal{F}} \hat{V}(a|R). \quad (1)$$

The final allocation $a_R^* \in \mathcal{F}$ and payments $p \in \mathbb{R}_+^n$ are computed based on the elicited reports R only. We assume that bidders' utilities are of the form $u_i(a, p) = v_i(a_i) - p_i$.

As the auctioneer can generally only query each bidder i a limited number of bundles $|R_i| \leq Q^{\max}$ (e.g., $Q^{\max} = 100$), the mechanism needs a sophisticated preference elicitation algorithm, with the goal of finding a highly efficient allocation a_R^* with a limited number of value queries.

2.2 A Machine Learning-powered ICA

We now review the *machine learning-powered combinatorial auction (MLCA)* by Brero, Lubin, and Seuken (2021).

At the core of MLCA is a *query module* (Algorithm 1), which, for each bidder $i \in I \subseteq N$, determines a new value query q_i . First, in the *estimation step* (Line 1), an ML algorithm \mathcal{A}_i is used to learn bidder i 's valuation from reports R_i . Next, in the *optimization step* (Line 2), an *ML-based WDP* is solved to find a candidate q of value queries. In principle, any ML algorithm \mathcal{A}_i that allows for solving the corresponding ML-based WDP in a fast way could be used. In this paper, we consider plain NNs as the ML algorithm \mathcal{A}_i a variation introduced by Weissteiner and Seuken (2020). See Weissteiner and Seuken (2020) for details on the NN-based *estimation* and *optimization step*. Finally, if q_i has already been queried before (Line 4), another, more restricted NN-based WDP (Line 6) is solved and q_i is updated correspondingly. This ensures that all final queries q are new.

Algorithm 1: NEXTQUERIES(I, R) (Brero et al. 2021)

Inputs: Index set of bidders I and reported values R

- 1 **foreach** $i \in I$ **do** Fit \mathcal{A}_i on R_i : $\mathcal{A}_i[R_i]$ ▷ Estimation step
- 2 Solve $q \in \operatorname{argmax}_{a \in \mathcal{F}} \sum_{i \in I} \mathcal{A}_i[R_i](a_i)$ ▷ Optimization step
- 3 **foreach** $i \in I$ **do**
- 4 **if** $q_i \in R_i$ **then** ▷ Bundle already queried
- 5 Define $\mathcal{F}' = \{a \in \mathcal{F} : a_i \neq x, \forall x \in R_i\}$
- 6 Re-solve $q' \in \operatorname{argmax}_{a \in \mathcal{F}'} \sum_{l \in I} \mathcal{A}_l[R_l](a_l)$
- 7 Update $q_i = q'_i$
- 8 **end**
- 9 **end**
- 10 **return** Profile of new queries $q = (q_1, \dots, q_n)$

In Algorithm 2, we present MLCA. MLCA proceeds in rounds until a maximum number of queries per bidder Q^{\max} is reached. In each round, it calls Algorithm 1 ($(Q^{\text{round}} - 1)n + 1$ times: for each bidder $i \in N$, $Q^{\text{round}} - 1$ times excluding a different bidder $j \neq i$ (Lines 5–10, sampled *marginal economies*) and once including all bidders (Line 11, *main*

Algorithm 2: MLCA($Q^{\text{init}}, Q^{\max}, Q^{\text{round}}$) (Brero et al. 2021)

Params: $Q^{\text{init}}, Q^{\max}, Q^{\text{round}}$ initial, max and #queries/round

- 1 **foreach** $i \in N$ **do**
- 2 Receive reports R_i for Q^{init} randomly drawn bundles
- 3 **end**
- 4 **for** $k = 1, \dots, \lfloor (Q^{\max} - Q^{\text{init}})/Q^{\text{round}} \rfloor$ **do** ▷ Round iterator
- 5 **foreach** $i \in N$ **do** ▷ Marginal economy queries
- 6 Draw uniformly without replacement $(Q^{\text{round}} - 1)$ bidders from $N \setminus \{i\}$ and store them in \tilde{N}
- 7 **foreach** $j \in \tilde{N}$ **do**
- 8 $q^{\text{new}} = q^{\text{new}} \cup \text{NextQueries}(N \setminus \{j\}, R_{-j})$
- 9 **end**
- 10 **end**
- 11 $q^{\text{new}} = \text{NextQueries}(N, R)$ ▷ Main economy queries
- 12 **foreach** $i \in N$ **do**
- 13 Receive reports R_i^{new} for q_i^{new} , set $R_i = R_i \cup R_i^{\text{new}}$
- 14 **end**
- 15 **end**
- 16 From reports R compute a_R^* as in (1) and VCG payments p
- 17 **return** Final allocation a_R^* and payments p

economy).¹ At the end of each round, the mechanism receives reports R^{new} from all bidders for the newly generated queries q^{new} , and updates the overall elicited reports R (Lines 12–14). In Line 16, MLCA computes an allocation a_R^* that maximizes the *reported* social welfare and computes VCG payments p based on the reported values.

Remark 1 (IR, No-Deficit, and Incentives of MLCA). Brero, Lubin, and Seuken (2021) showed that MLCA satisfies individual rationality and no-deficit, with any ML algorithm \mathcal{A}_i . Furthermore, they studied the incentive properties of MLCA; this is important, given that opportunities for manipulations might lower efficiency. Like all deployed spectrum auctions (including the CCA (Ausubel and Baranov 2017)) MLCA is not strategyproof. However, Brero, Lubin, and Seuken (2021) argued that it has good incentives in practice; and given two additional assumptions, bidding truthfully is an ex-post Nash equilibrium in MLCA. Their analyses apply to MLCA using any ML algorithm, and therefore also to an MVNN-based MLCA. We present a more detailed summary of their incentive analysis in Appendix A.

3 Monotone-Value Neural Networks

In combinatorial assignment problems, value functions are used to model each agent's (reported) value for a bundle of items ($\hat{v}_i : \{0, 1\}^m \rightarrow \mathbb{R}_+$). However, while the bundle space grows exponentially with the number of items, the agents' value functions often exhibit useful structure that can be exploited. A common assumption is monotonicity:

(M) Monotonicity (“additional items increase value”):

For $A, B \in 2^M$: if $A \subseteq B$ it holds that $\hat{v}_i(A) \leq \hat{v}_i(B)$.

This property is satisfied in many market domains. For example, in many CAs (where this property is called *free disposal*, bidders can freely dispose of unwanted items; in combinatorial course allocation, students can just drop courses

¹In total each bidder is queried Q^{round} bundles per round in MLCA.

they have been assigned. However, prior work on ML-based market design (Weissteiner and Seuken 2020; Weissteiner et al. 2020; Brero, Lubin, and Seuken 2021) has not taken this property into account, which negatively affects the performance (see Sections 4 and 5).

For ease of exposition, we additionally assume that the value functions are normalized:

(N) Normalization ("no value for empty bundle"):

$$\hat{v}_i(\emptyset) = \hat{v}_i((0, \dots, 0)) := 0$$

Note that this property is not required by our method and can be easily adapted to be any other fixed value, or to be a learned parameter. In the following, we denote with

$$\mathcal{V} := \{\hat{v}_i : \mathcal{X} \rightarrow \mathbb{R}_+ \mid \text{satisfy (N) and (M)}\} \quad (2)$$

the set of all value functions, that satisfy the *normalization* and *monotonicity* property. Next, we introduce *Monotone-Value Neural Networks* (MVNNs) and show that they span the entire set \mathcal{V} . Thus, MVNNs are specifically suited to all applications with monotone value functions.

Definition 1 (MVNN). A MVNN $\mathcal{N}_i^\theta : \mathcal{X} \rightarrow \mathbb{R}_+$ for bidder $i \in N$ is defined as

$$\mathcal{N}_i^\theta(x) = W^{i,K_i} \varphi_{0,t}(\dots \varphi_{0,t}(W^{i,1}x + b^{i,1}) \dots), \quad (3)$$

- $K_i \in \mathbb{N}$ is the number of layers ($K_i - 2$ hidden layers),
- $\varphi_{0,t}$ is our MVNN-specific activation function with cutoff $t > 0$, which we call bounded ReLU (bReLU):

$$\varphi_{0,t}(z) := \begin{cases} 0, & z \leq 0 \\ z, & 0 \leq z \leq t \\ t, & t \leq z \end{cases} \quad (4)$$

- $W^i := (W^{i,k})_{k=1}^{K_i}$ with $W^{i,k} \geq 0$ and $b^i := (b^{i,k})_{k=1}^{K_i}$ with $b^{i,k} \leq 0$ denote a tuple of non-negative weights and non-positive biases of dimensions $d^{i,k} \times d^{i,k-1}$ and $d^{i,k}$, whose parameters are stored in $\theta = (W^i, b^i)$.²

Unless explicitly stated, we consider in the following a cutoff of $t = 1$ for the bReLU. Then $\varphi(z) := \varphi_{0,1}(z) = \min(1, \max(0, z))$ is a discretized version of the popular sigmoid activation function $z \mapsto (1 + e^{-t})^{-1}$. We will use this discretization property to encode our MVNNs as MIPs.

3.1 Theoretical Analysis and MIP-Formulation

Next, we provide a theoretical analysis of MVNNs and present a MIP formulation.

Lemma 1. Let $\mathcal{N}_i^\theta : \mathcal{X} \rightarrow \mathbb{R}_+$ denote a MVNN from Definition 1. Then it holds that \mathcal{N}_i^θ fulfills (N) and (M), i.e. $\mathcal{N}_i^{(W^i, b^i)} \in \mathcal{V}$ for all $W^i \geq 0$ and $b^i \leq 0$.

We provide the proof for Lemma 1 in Appendix B.1. Next, we state our main theorem about MVNNs.

²We apply a linear readout map to the last hidden layer, i.e., no $\varphi_{0,t}$ and $b^{i,K_i} := 0$. By setting $b^{i,K_i} \neq 0$ with *trainable=False*, the MVNN can model any other value than zero in the normalization property. By not restricting $b^{i,k} \leq 0$ and setting $b^{i,K_i} \neq 0$ with *trainable=True* one can also learn the value for the empty bundle.

Theorem 1 (Universality). Any value function $\hat{v}_i : \mathcal{X} \rightarrow \mathbb{R}_+$ that satisfies (N) and (M) can be represented exactly as a MVNN \mathcal{N}_i^θ from Definition 1, i.e.,

$$\mathcal{V} = \left\{ \mathcal{N}_i^{(W^i, b^i)} : W^i \geq 0, b^i \leq 0 \right\}. \quad (5)$$

We present a constructive proof for Theorem 1 in Appendix B.2. In the proof, we consider an arbitrary $(\hat{v}_i(x))_{x \in \mathcal{X}} \in \mathcal{V}$ for which we construct a two hidden layer MVNN \mathcal{N}_i^θ of dimensions $[m, 2^m - 1, 2^m - 1, 1]$ with parameters $\theta = (W_{\hat{v}_i}^i, b_{\hat{v}_i}^i)$ such that $\mathcal{N}_i^\theta(x) = \hat{v}_i(x) \forall x \in \mathcal{X}$.

Table 1 illustrates how we can capture complementarities, substitutabilities and independent items via a MVNN.

Example 1 (MVNN). Consider the set of items $M = \{x_1, x_2, x_3\}$ and the associated (reported) value function \hat{v}_i shown in Table 1 (where we use 001 as a shorthand notation for $(0, 0, 1)$):

	000	100	010	001	110	101	011	111
\hat{v}_i	0	1	1	1	1	3	2	3

Table 1: Example on flexibility of MVNNs.

In this example, x_1 and x_2 are substitutes, i.e., $2 = \hat{v}_i(\{x_1\}) + \hat{v}_i(\{x_2\}) > \hat{v}_i(\{x_1, x_2\}) = 1$; x_1 and x_3 are complements, i.e., $2 = \hat{v}_i(\{x_1\}) + \hat{v}_i(\{x_3\}) < \hat{v}_i(\{x_1, x_3\}) = 3$; and x_2 and x_3 are independent, i.e., $2 = \hat{v}_i(\{x_2\}) + \hat{v}_i(\{x_3\}) > \hat{v}_i(\{x_2, x_3\}) = 1$. This reported value function can be exactly captured by a MVNN $\mathcal{N}_i^\theta(x)$ in the following way:

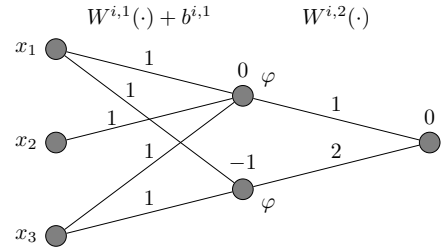


Figure 1: MVNN \mathcal{N}_i^θ with $\mathcal{N}_i^\theta(x) = \hat{v}_i(x) \quad \forall x \in \mathcal{X}$.

Biases are marked at the top of each neuron and weights are marked above the corresponding connections. A missing connection denotes a weight of 0. We see that the second kink (at $t = 1$) of the bReLU together with the 0 bias of the top neuron in the hidden layer implements the substitutability between x_1 and x_2 . Furthermore, the complementarity between x_1 and x_2 is implemented by the bottom neuron in the hidden layer via the negative bias -1 and the first kink (at 0) of the bReLU.

A key step in combinatorial assignment mechanisms is finding the social welfare-maximizing allocation, i.e., solving the *Winner Determination Problem* (WDP). To use MVNNs in such mechanisms, we need to be able to efficiently solve the MVNN-based WDP. To this end, we show how to formulate the MVNN-based WDP as a MIP. First, we show how to encode one hidden layer of an MVNN as multiple linear constraints. We provide the proof in Appendix B.3.

Lemma 2. Fix bidder $i \in N$, let $k \in \{2, \dots, K_i - 1\}$ and denote the pre-activated output of the k^{th} hidden layer as $o^{i,k} := W^{i,k-1} z^{i,k-1} + b^{i,k-1}$ with $W^{i,k-1} \in \mathbb{R}^{d_k^i \times d_{k-1}^i}$, $b^{i,k-1} \in \mathbb{R}^{d_k^i}$. Then the value of the k^{th} hidden layer $z^{i,k} := \varphi(o^{i,k}) = \min(1, \max(0, o^{i,k})) = -\max(-1, -\eta^{i,k})$, with $\eta^{i,k} := \max(0, o^{i,k})$ can be equivalently expressed by the following linear constraints:

$$o^{i,k} \leq \eta^{i,k} \leq o^{i,k} + y^{i,k} \cdot L_1^{i,k} \quad (6)$$

$$0 \leq \eta^{i,k} \leq (1 - y^{i,k}) \cdot L_2^{i,k} \quad (7)$$

$$\eta^{i,k} - \mu^{i,k} \cdot L_3^{i,k} \leq z^{i,k} \leq \eta^{i,k} \quad (8)$$

$$1 - (1 - \mu^{i,k}) \cdot L_4^{i,k} \leq z^{i,k} \leq 1 \quad (9)$$

$$y^{i,k} \in \{0, 1\}^{d_k^i}, \quad \mu^{i,k} \in \{0, 1\}^{d_k^i}, \quad (10)$$

where $L_1^{i,k}, L_2^{i,k}, L_3^{i,k}, L_4^{i,k} \in \mathbb{R}_+$ are large enough constants for the respective big-M constraints.

Finally, we formulate the MVNN-based WDP as a MIP.

Theorem 2 (MIP). Using the notation of Lemma 2, it holds that the MVNN-based WDP $\max_{a \in \mathcal{F}} \sum_{i \in N} \mathcal{N}_i^{(W^i, b^i)}(a_i)$ can be equivalently formulated as the following MIP:

$$\max_{a \in \mathcal{F}, z^{i,k}, \mu^{i,k}, \eta^{i,k}, y^{i,k}} \left\{ \sum_{i \in N} W^{i, K_i} z^{i, K_i - 1} \right\} \quad (11)$$

s.t. for $i \in N$ and $k \in \{2, \dots, K_i - 1\}$

$$z^{i,1} = a_i \quad (12)$$

$$W^{i,k-1} z^{i,k-1} + b^{i,k-1} \leq \eta^{i,k} \quad (13)$$

$$\eta^{i,k} \leq W^{i,k-1} z^{i,k-1} + b^{i,k-1} + y^{i,k} \cdot L_1^{i,k} \quad (14)$$

$$0 \leq \eta^{i,k} \leq (1 - y^{i,k}) \cdot L_2^{i,k} \quad (15)$$

$$\eta^{i,k} - \mu^{i,k} \cdot L_3^{i,k} \leq z^{i,k} \leq \eta^{i,k} \quad (16)$$

$$1 - (1 - \mu^{i,k}) \cdot L_4^{i,k} \leq z^{i,k} \leq 1 \quad (17)$$

$$y^{i,k} \in \{0, 1\}^{d_k^i}, \quad \mu^{i,k} \in \{0, 1\}^{d_k^i} \quad (18)$$

Proof. The proof follows by iteratively applying Lemma 2 for each bidder and all her respective hidden layers. \square

The MIP from Theorem 2 can be solved via standard optimization packages like CPLEX³.

Fact 1. One can significantly reduce the solve time for the MIPs in Theorem 2 by removing unnecessary constraints via tightening the bounds of each neuron as much as possible. In Appendix B.4, we present the details of our bound tightening approach, applying interval arithmetic (Tjeng, Xiao, and Tedrake 2019) to MVNNs. For a plain ReLU NN, these IA bounds are not tight and calculating tighter bounds in a computationally efficient manner is very challenging. However, for MVNNs, the IA bounds are always perfectly tight, because of their encoded monotonicity property. The upper bound of a neuron is the value the neuron outputs for the

input $x = (1, 1, \dots, 1)$ and the lower bound is the corresponding value for the input $x = (0, 0, \dots, 0)$. This is a big advantage of MVNN-based MIPs compared to plain (ReLU) NN-based MIPs.

Remark 2 (MVNNs as Preference Generator). To experimentally evaluate a new mechanism one needs to generate many different possible value functions. Preference generators like the Spectrum Auction Test Suite (Weiss, Lubin, and Seuken 2017) are carefully designed to capture the essential properties of spectrum auctions, but they are not universally applicable and do not cover every possible market scenario. Moreover, in some settings, no task-specific simulation engines are even available. Instead of using such a domain-specific preference generator, one can also use MVNNs with randomly initialized weights to generate possible value functions. An advantage of random MVNNs is that they are universal (see Theorem 1) and hence come with a diversity rich enough to sample any possible monotone value function with arbitrarily complex substitutabilities and complementarities (the distribution of supplements and complements can be controlled via the cutoff t , where the smaller/larger t the more substitutabilities/complementarities). These types of generative test beds become increasingly important in the ML-community to avoid overfitting on specific simulation engines and/or real data sets (Osband et al. 2021).

3.2 Implementation of MVNNs

We briefly discuss how to implement MVNNs, as care must be taken in various steps. We use PYTORCH 1.8.1.

Recall that the three key building blocks of MVNNs are the bReLU φ , the (element-wise) non-negative weights W^i , and the (element-wise) non-positive biases b^i . The bReLU φ can be straightforwardly implemented as a custom activation function in PYTORCH. However, the constraints on the weights and biases can be implemented in several different ways. To simplify the exposition, we here only describe the method we call MVNN-RELU-PROJECTED, as we have found experimentally that this method performs best. However, the other options we have explored may be of independent interest to some readers, and we therefore provide a detailed discussion of them in Appendix B.5.

In MVNN-RELU-PROJECTED, we project W^i and b^i prior to every forward pass to be non-negative and non-positive, respectively, using ReLU $z \mapsto \pm \max(0, \pm z)$. Thus, (in contrast to some of the other methods we explored), gradient descent (GD) updates are performed on the already transformed weights and biases and we do not differentiate through the ReLUs. After the last GD step, we apply post-processing and project W^i and b^i again via $z \mapsto \pm \max(0, \pm z)$.

Remark 3. For applications where value functions are expected to be "almost" (but not completely) monotone, one can easily adapt MVNNs to only have soft monotonicity constraints by implementing the inequality constraints on the weights and biases via regularization, e.g., regularizing via $\sum_{i,k,j,l} \max(0, -W_{j,l}^{i,k})$. This results in soft-MVNNs that can model non-monotone changes in some items if the data evidence is strong.

³To account for a general cutoff $t \neq 1$ in the bReLU, one needs to adjust (9) and (17) by replacing the left- and rightmost 1 with t .

4 Prediction Performance of MVNNs

In this section, we show that in all considered CA domains, MVNNs are significantly better at capturing bidders’ complex value functions than plain (ReLU) NNs, which allows them to extrapolate much better in the bundle space.

4.1 Experimental Setup - Prediction Performance

CA Domains For the experimental evaluation, we use simulated data from the Spectrum Auction Test Suite (SATS) (Weiss, Lubin, and Seuken 2017). We consider the following four domains:

- **The Global Synergy Value Model (GSVM)** (Goeree and Holt 2010) has 18 items, 6 *regional* and 1 *national bidder*.
- **The Local Synergy Value Model (LSVM)** (Scheffell, Ziegler, and Bichler 2012) consists of 18 items, 5 *regional* and 1 *national bidder*. Complementarities arise from spatial proximity of items.
- **The Single-Region Value Model (SRVM)** (Weiss, Lubin, and Seuken 2017) has 29 items and 7 bidders (categorized as *local*, *high frequency regional*, or *national*) and models large UK 4G spectrum auctions.
- **The Multi-Region Value Model (MRVM)** (Weiss, Lubin, and Seuken 2017) has 98 items and 10 bidders (categorized as *local*, *regional*, or *national*) and models large Canadian 4G spectrum auctions.

When simulating bidders, we follow prior work (e.g., Brero, Lubin, and Seuken (2021)) and assume truthful bidding (i.e., $\hat{v}_i = v_i$). Details on how we collect the data and the train/val/test split can be found in Appendix C.1.

HPO To efficiently and fairly optimize the hyperparameters of MVNNs and plain NNs for best generalization across different instances of each SATS domain, we frame the *hyper parameter optimization (HPO)* problem as an algorithm configuration problem and use the well-established *sequential model-based algorithm configuration (SMAC)* (Hutter, Hoos, and Leyton-Brown 2011). SMAC quickly discards hyperparameters which already perform poorly on a few instances and proposes more promising ones via Bayesian optimization. It is flexible enough for the parameterization of NNs as it naturally handles a mixture of categorical, integer and float hyperparameters. We optimize the following hyperparameters: *architecture* (number of hidden layers and nodes), *epochs*, *batch size*, *optimizer* and corresponding *learning rate*, *L2-regularization*, and *loss function*. Further details on the setting including hyperparameter ranges can be found in Appendix C.2.

4.2 Prediction Performance Results

For ease of exposition, we only present our results for the MVNN-RELU-PROJECTED implementation of our MVNNs (simply termed MVNN in the following). Results for other MVNN implementations can be found in the Appendix C.3. In Table 2, we compare the prediction performance of the winning models that the HPO found for different amounts of training data (T) on the test data. We see that, compared to plain NNs, MVNNs provide both a significantly better fit in terms of Pearson correlation r_{xy} (i.e., cardinal values are better captured) as well as a better Kendall

DOMAIN	T	BIDDER	$r_{xy} \uparrow$		KT \uparrow	
			MVNN	NN	MVNN	NN
GSVM	10	NAT	0.856 \pm 0.022	0.782 \pm 0.020	0.668 \pm 0.027	0.583 \pm 0.021
		REG	0.816 \pm 0.034	0.746 \pm 0.033	0.633 \pm 0.038	0.557 \pm 0.033
	20	NAT	0.965 \pm 0.007	0.911 \pm 0.017	0.849 \pm 0.017	0.752 \pm 0.029
		REG	0.973 \pm 0.009	0.944 \pm 0.011	0.882 \pm 0.020	0.815 \pm 0.021
	50	NAT	0.997 \pm 0.000	0.995 \pm 0.000	0.962 \pm 0.003	0.953 \pm 0.003
		REG	0.999 \pm 0.000	0.995 \pm 0.001	0.974 \pm 0.002	0.953 \pm 0.003
LSVM	10	NAT	0.598 \pm 0.019	0.701 \pm 0.013	0.693 \pm 0.011	0.710 \pm 0.023
		REG	0.785 \pm 0.028	0.679 \pm 0.027	0.605 \pm 0.031	0.504 \pm 0.025
	50	NAT	0.796 \pm 0.012	0.681 \pm 0.024	0.753 \pm 0.009	0.678 \pm 0.035
		REG	0.963 \pm 0.007	0.938 \pm 0.006	0.860 \pm 0.017	0.812 \pm 0.013
	100	NAT	0.834 \pm 0.008	0.719 \pm 0.015	0.813 \pm 0.005	0.706 \pm 0.018
		REG	0.983 \pm 0.005	0.969 \pm 0.005	0.918 \pm 0.015	0.857 \pm 0.012
SRVM	10	H.F.	0.795 \pm 0.018	0.762 \pm 0.011	0.626 \pm 0.020	0.607 \pm 0.012
		LO	0.660 \pm 0.029	0.570 \pm 0.030	0.559 \pm 0.030	0.489 \pm 0.032
		NAT	0.676 \pm 0.032	0.636 \pm 0.018	0.560 \pm 0.026	0.535 \pm 0.012
		REG	0.693 \pm 0.027	0.675 \pm 0.020	0.562 \pm 0.023	0.544 \pm 0.014
	50	H.F.	0.933 \pm 0.007	0.895 \pm 0.012	0.853 \pm 0.013	0.803 \pm 0.020
		LO	0.955 \pm 0.008	0.794 \pm 0.019	0.902 \pm 0.000	0.771 \pm 0.030
		NAT	0.995 \pm 0.002	0.916 \pm 0.008	0.918 \pm 0.005	0.801 \pm 0.009
		REG	0.995 \pm 0.001	0.945 \pm 0.017	0.931 \pm 0.004	0.823 \pm 0.022
	100	H.F.	0.956 \pm 0.004	0.927 \pm 0.005	0.908 \pm 0.006	0.896 \pm 0.006
		LO	0.978 \pm 0.006	0.872 \pm 0.003	0.903 \pm 0.000	0.900 \pm 0.002
		NAT	0.999 \pm 0.000	0.959 \pm 0.004	0.952 \pm 0.003	0.841 \pm 0.008
		REG	0.981 \pm 0.033	0.975 \pm 0.002	0.948 \pm 0.021	0.895 \pm 0.012
MRVM	10	LO	0.383 \pm 0.023	0.296 \pm 0.021	0.262 \pm 0.017	0.200 \pm 0.015
		NAT	0.529 \pm 0.022	0.597 \pm 0.009	0.365 \pm 0.018	0.414 \pm 0.008
		REG	0.459 \pm 0.031	0.368 \pm 0.052	0.322 \pm 0.022	0.255 \pm 0.038
	100	LOCAL	0.918 \pm 0.012	0.729 \pm 0.012	0.786 \pm 0.019	0.545 \pm 0.012
		NAT	0.887 \pm 0.011	0.776 \pm 0.010	0.726 \pm 0.014	0.581 \pm 0.010
		REG	0.917 \pm 0.015	0.747 \pm 0.016	0.779 \pm 0.027	0.572 \pm 0.018
	300	LOCAL	0.972 \pm 0.003	0.934 \pm 0.005	0.883 \pm 0.010	0.819 \pm 0.009
		NAT	0.933 \pm 0.008	0.927 \pm 0.014	0.814 \pm 0.009	0.808 \pm 0.013
		REG	0.958 \pm 0.009	0.923 \pm 0.005	0.851 \pm 0.019	0.809 \pm 0.012
		REG	0.958 \pm 0.009	0.923 \pm 0.005	0.851 \pm 0.019	0.809 \pm 0.012

Table 2: Prediction performance measured via Pearson correlation coefficient (r_{xy}) and Kendall tau (KT) with a 95%-CI in four SATS domains with corresponding bidder types: high frequency (H.F.), local (LO), regional (REG) and national (NAT), averaged over 30 auction instances. Both MVNNs and plain NNs are trained on T and evaluated on 209 715 – T random bundles. Winners are marked in grey.

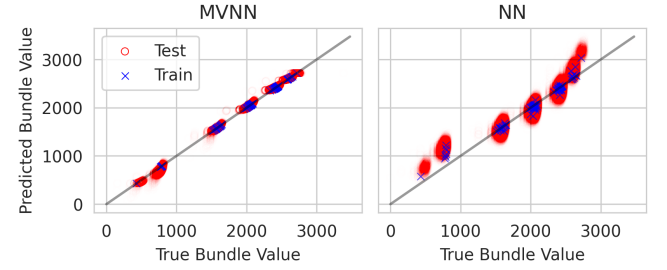


Figure 2: Prediction performance of MVNNs vs plain NNs in SRVM for the national bidder. The identity is shown in grey. Points are plotted semi-transparently.

Tau rank correlation KT (i.e., a better ordinal ranking). Thus, enforcing the monotonicity property in MVNNs significantly improves the learning performance.

Figure 2 illustrates our findings by providing a visual comparison of the prediction performance results for the SRVM domain.⁴ We see that the MVNN fits the training data exactly (blue crosses), although HPO only optimized generalization performance on the validation data. This is a strong indication that MVNNs correspond to a more realis-

⁴We provide corresponding plots for the other domains and bidder types in Appendix C.3; the results are qualitatively similar.

DOMAIN	Q^{INIT}	Q^{ROUND}	Q^{MAX}	EFFICIENCY LOSS IN % \downarrow			T-TEST FOR EFFICIENCY: $\mathcal{H}_0 : \mu_{\text{NN}} \leq \mu_{\text{MVNN}}$
				MVNN	NN	RS	
GSVM	40	4	100	00.00 \pm 0.00	00.00 \pm 0.00	30.34 \pm 1.61	
LSVM	40	4	100	00.70 \pm 0.40	02.91 \pm 1.44	31.73 \pm 2.15	$p_{\text{VAL}} = 2\text{e}-03$
SRVM	40	4	100	00.23 \pm 0.06	01.13 \pm 0.22	28.56 \pm 1.74	$p_{\text{VAL}} = 5\text{e}-10$
MRVM	40	4	100	08.16 \pm 0.41	09.05 \pm 0.53	48.79 \pm 1.13	$p_{\text{VAL}} = 9\text{e}-03$

Table 3: Efficiency loss of MLCA with MVNNs vs MLCA with plain NNs and random search (RS). Shown are averages and a 95% CI on a test set of 50 CA instances. Winners based on a (paired) t-test with significance level of 1% are marked in grey.

tic prior, since for a realistic prior, it is optimal to perfectly fit the training data in noiseless settings (Heiss et al. 2021, Proposition D.2.a). In contrast, the HPO has selected hyperparameters for the plain NNs that result in a worse fit of the training data (otherwise generalization to unseen data would be even worse). Moreover, the plain NNs show a particularly bad fit on the lower and higher valued bundles, which are less frequent in the training data.

5 MVNN-based Iterative CA

To evaluate the perform of MVNNs when used inside a combinatorial market mechanism, we have integrated MVNNs into the MLCA mechanism, yielding an *MVNN-powered Iterative Combinatorial Auction*. In this Section, we compare the economic efficiency of our MVNN-based MLCA against the previously proposed NN-based MLCA. For solving the MVNN-based WDPs in MLCA, we use our MIP formulation from Theorem 2.

5.1 Experimental Setup - MLCA

To generate synthetic CA instances, we use the same four SATS domains we have studied in Section 4. SATS also gives us access to the true optimal allocation a^* , which we use to measure the *efficiency loss*, i.e., $1 - V(a)/V(a^*)$ and *relative revenue* $\sum_{i \in N} p_i/V(a^*)$ of an allocation $a \in \mathcal{F}$ found by MLCA. Due to the long run-time of a single evaluation of MLCA and the necessity to evaluate many CA instances to arrive at statistically significant results, we perform a restricted HPO, which only uses, for each domain, as incumbents the winners of the prediction performance experiment (Table 2) for the three amounts of training data T . This is a reasonable choice, because in the prediction performance we optimize the generalization performance for bidders' value functions that is also key in MLCA.

For each domain, we use $Q^{\text{init}} = 40$ initial random queries and set the query budget to $Q^{\text{max}} = 100$. We terminate MLCA in an intermediate iteration if it already found an efficient allocation (i.e., with 0 efficiency loss).

Following prior work (Brero, Lubin, and Seuken 2021) we set $Q^{\text{round}} = 4$, i.e., in each iteration of MLCA we ask each bidder 1 query in the main economy (including all bidders) and 3 queries from randomly sampled marginal economies (excluding one bidder). This choice ensures a trade-off between efficiency (more main economy queries decrease the efficiency loss) and revenue (more marginal queries increase revenue).

5.2 Efficiency Results

In Table 3, we present the efficiency results of MVNN-based MLCA and NN-based MLCA, averaged over 50 auction instances. We focus on efficiency rather than revenue, since spectrum auctions are government-run auctions with a mandate to maximize efficiency and not revenue (Cramton 2013). In Appendices D.2 and D.3 we also present revenue results and a detailed discussion on revenue.

For each domain, we present results corresponding to the best MVNNs and NNs amongst the three incumbents obtained from the prediction performance experiments. We present detailed results for all three incumbents in Appendix D.2. Overall, we see that the better prediction performance of MVNNs (Table 2) indeed translates to smaller efficiency losses in MLCA. In LSVM and SRVM, MVNNs significantly outperform NNs and have on average a more than four times lower efficiency loss. In MRVM, MVNN's average efficiency loss is approximately 1% point smaller than the NN's loss. Given that in the 2014 Canadian 4G auction the total revenue was on the order of 5 billion USD (Ausubel and Baranov 2017), an efficiency loss decrease of 1% point in MRVM can translate to welfare gains on the order of 50 million USD. Finally, in GSVM, the simplest domain, where bidders' value functions have at most two-way interactions between items, both MVNNs and plain NNs incur no efficiency loss. As a baseline, we present random search (RS), where all queries for each bidder are drawn i.i.d. uniformly at random from the bundle space. We observe that RS incurs efficiency losses of 30% to 50% across the four domains, which illustrates the need for careful preference elicitation and highlights the strength of ML-based mechanisms.

In Figure 3, we present the efficiency loss path (i.e., the regret curve) corresponding to Table 3. We see that in LSVM and SRVM, MVNNs lead to a smaller (average) efficiency loss for *every* number of queries. In MRVM, the same holds true for 50 and more queries. In GSVM, both networks have no efficiency loss in every instance after only 56 queries. Since a single query can be very costly in real-world CAs, it makes sense to ask few queries. Figure 3 shows that in LSVM, SRVM and MRVM, MVNNs consistently outperform plain NNs also in settings with a small number of queries.

5.3 MIP Runtime Analysis

Recall that, when integrating MVNNs into MLCA or another iterative combinatorial assignment mechanism, one needs to solve the MVNN-based WDP multiple times in one full run of the mechanism. For example, in one MLCA

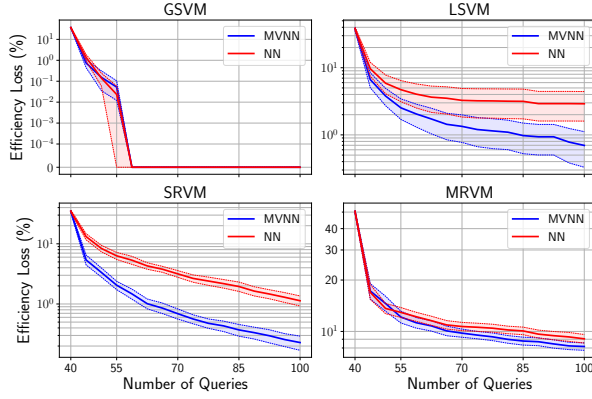


Figure 3: Efficiency loss paths of MLCA with MVNNs vs plain NNs in all domains. Shown are averages with 95% CIs over 50 auction instances.

run, thousands of MVNN-based WDPs are solved. Thus, the key computational challenge when integrating MVNNs in such mechanisms is to efficiently solve the MVNN-based WDP. In Theorem 2, we have shown how to reformulate the MVNN-based WDP into a MIP, which can be solved efficiently for moderate architectures sizes. However, due to the bReLU activation function, i.e., the two cutoffs at 0 and $t > 0$, the MVNN-based MIP has twice the number of binary variables ($y^{i,k}$ and $\mu^{i,k}$) than the MIP encoding of a plain NN with ReLUs (Weissteiner and Seuken 2020). To study the impact of those design features on the overall runtime, we have conducted a series of runtime experiments, comparing the MVNN-based and the NN-based MIP.

Figure 4 presents the MIP runtime results for selected architectures. We observe two effects: First, even though the MVNN-based MIPs have twice the number of binary variables, they can be solved faster than the plain NN-based MIPs for all architectures. Second, the deeper the architecture or the more neurons, the larger the difference in runtime becomes. One possible explanation for both effects is that MVNNs are more regular than plain NNs (due to their monotonicity property) and are thus easier to optimize.

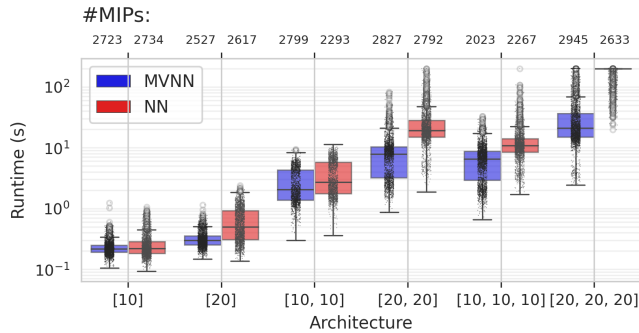


Figure 4: MIP runtime (200s time limit) of MVNNs vs plain NNs in MLCA on 10 LSVM instances for a selection of architectures (hidden layers) with different depth and neurons.

6 Conclusion

In this paper, we have introduced MVNNs, a new class of NNs that is specifically designed to model normalized and monotone value functions in combinatorial assignment problems. We have experimentally evaluated the performance of MVNNs in four combinatorial spectrum auction domains and shown that they yield superior performance compared to plain NNs with respect to prediction performance, economic efficiency, and runtime. Thus, incorporating important structural knowledge in the ML algorithm plays an important role in combinatorial assignment.

MVNNs enable us to incorporate an informative *prior* into a market mechanism. Future work could use such informative priors and enhance existing mechanisms (e.g., MLCA) by also using the *posterior* estimates in a more principled way than just the mean prediction. For example, one could frame an ICA as a (combinatorial) Bayesian optimization problem and integrating a well-defined notion of posterior uncertainty to foster exploration (Heiss et al. 2021). Finally, it would be interesting to also evaluate the performance of MVNNs in other combinatorial assignment problems such as combinatorial exchanges and course allocation.

7 Acknowledgments

This paper is part of a project that has received funding from the European Research Council (ERC) under the European Union’s Horizon 2020 research and innovation programme (Grant agreement No. 805542). This material is based upon work supported by the National Science Foundation under grant no. CMMI-1761163.

References

- Ausubel, L.; and Cramton, P. 2011. Auction design for wind rights. *Report to Bureau of Ocean Energy Management, Regulation and Enforcement*.
- Ausubel, L. M.; and Baranov, O. 2017. A practical guide to the combinatorial clock auction. *Economic Journal*, 127(605): F334–F350.
- Ausubel, L. M.; Cramton, P.; and Milgrom, P. 2006. The clock-proxy auction: A practical combinatorial auction design. In Cramton, P.; Shoham, Y.; and Steinberg, R., eds., *Combinatorial Auctions*, 115–138. MIT Press.
- Bichler, M.; Fux, V.; and Goeree, J. K. 2019. Designing combinatorial exchanges for the reallocation of resource rights. *Proceedings of the National Academy of Sciences*, 116(3): 786–791.
- Blum, A.; Jackson, J.; Sandholm, T.; and Zinkevich, M. 2004. Preference elicitation and query learning. *Journal of Machine Learning Research*, 5: 649–667.
- Brero, G.; Lahaie, S.; and Seuken, S. 2019. Fast Iterative Combinatorial Auctions via Bayesian Learning. In *Proceedings of the 33rd AAAI Conference of Artificial Intelligence*.
- Brero, G.; Lubin, B.; and Seuken, S. 2018. Combinatorial Auctions via Machine Learning-based Preference Elicitation. In *Proceedings of the 27th International Joint Conference on Artificial Intelligence*.

Brero, G.; Lubin, B.; and Seuken, S. 2021. Machine Learning-powered Iterative Combinatorial Auctions. *arXiv preprint arXiv:1911.08042*.

Bronstein, M. M.; Bruna, J.; LeCun, Y.; Szlam, A.; and Vandergheynst, P. 2017. Geometric deep learning: going beyond euclidean data. *IEEE Signal Processing Magazine*, 34(4): 18–42.

Budish, E. 2011. The combinatorial assignment problem: Approximate competitive equilibrium from equal incomes. *Journal of Political Economy*, 119(6): 1061–1103.

Cramton, P. 2013. Spectrum auction design. *Review of Industrial Organization*, 42(2): 161–190.

Dütting, P.; Feng, Z.; Narasimhan, H.; Parkes, D. C.; and Ravindranath, S. S. 2019. Optimal auctions through deep learning. In *Proceedings of the 36th International Conference on Machine Learning*.

Goeree, J. K.; and Holt, C. A. 2010. Hierarchical package bidding: A paper & pencil combinatorial auction. *Games and Economic Behavior*, 70(1): 146–169.

Heiss, J.; Weisstainer, J.; Wutte, H.; Seuken, S.; and Teichmann, J. 2021. NOMU: Neural Optimization-based Model Uncertainty. *arXiv preprint arXiv:2102.13640*.

Hutter, F.; Hoos, H. H.; and Leyton-Brown, K. 2011. Sequential model-based optimization for general algorithm configuration. In *International conference on learning and intelligent optimization*, 507–523. Springer.

Lahaie, S. M.; and Parkes, D. C. 2004. Applying learning algorithms to preference elicitation. In *Proceedings of the 5th ACM Conference on Electronic Commerce*.

Liu, X.; Han, X.; Zhang, N.; and Liu, Q. 2020. Certified monotonic neural networks. *arXiv preprint arXiv:2011.10219*.

Loshchilov, I.; and Hutter, F. 2017. SGDR: Stochastic Gradient Descent with Warm Restarts. *arXiv: Learning*.

Nisan, N.; and Segal, I. 2006. The communication requirements of efficient allocations and supporting prices. *Journal of Economic Theory*, 129(1): 192–224.

Osband, I.; Wen, Z.; Asghari, M.; Ibrahimi, M.; Lu, X.; and Van Roy, B. 2021. Epistemic Neural Networks. *arXiv preprint arXiv:2107.08924*.

Paszke, A.; Gross, S.; Massa, F.; Lerer, A.; Bradbury, J.; Chanan, G.; Killeen, T.; Lin, Z.; Gimelshein, N.; Antiga, L.; Desmaison, A.; Kopf, A.; Yang, E.; DeVito, Z.; Raison, M.; Tejani, A.; Chilamkurthy, S.; Steiner, B.; Fang, L.; Bai, J.; and Chintala, S. 2019. PyTorch: An Imperative Style, High-Performance Deep Learning Library. In Wallach, H.; Larochelle, H.; Beygelzimer, A.; d’Alché-Buc, F.; Fox, E.; and Garnett, R., eds., *Advances in Neural Information Processing Systems 32*, 8024–8035. Curran Associates, Inc.

Rahme, J.; Jelassi, S.; Bruna, J.; and Weinberg, S. M. 2020. A Permutation-Equivariant Neural Network Architecture For Auction Design. *arXiv preprint arXiv:2003.01497*.

Scheffel, T.; Ziegler, G.; and Bichler, M. 2012. On the impact of package selection in combinatorial auctions: an experimental study in the context of spectrum auction design. *Experimental Economics*, 15(4): 667–692.

Sill, J. 1998. Monotonic networks.

Tjeng, V.; Xiao, K. Y.; and Tedrake, R. 2019. Evaluating Robustness of Neural Networks with Mixed Integer Programming. In *International Conference on Learning Representations*.

Wehenkel, A.; and Louppe, G. 2019. Unconstrained monotonic neural networks. *Advances in Neural Information Processing Systems*, 32: 1545–1555.

Weiss, M.; Lubin, B.; and Seuken, S. 2017. Sats: A universal spectrum auction test suite. In *Proceedings of the 16th Conference on Autonomous Agents and MultiAgent Systems*, 51–59.

Weisstainer, J.; and Seuken, S. 2020. Deep Learning-powered Iterative Combinatorial Auctions. In *Proceedings of the 34th AAAI Conference of Artificial Intelligence*, 2284–2293.

Weisstainer, J.; Wendler, C.; Seuken, S.; Lubin, B.; and Püschel, M. 2020. Fourier Analysis-based Iterative Combinatorial Auctions. *arXiv preprint arXiv:2009.10749*.

You, S.; Ding, D.; Canini, K.; Pfeifer, J.; and Gupta, M. 2017. Deep Lattice Networks and Partial Monotonic Functions. *arXiv:1709.06680*.

Appendix

A Incentives of MLCA

In this Section, we briefly review the key arguments by [Brero, Lubin, and Seuken \(2021\)](#) why MLCA has good incentives in practice. First, we define VCG-payments given bidder’s reports.

Definition 2. (VCG PAYMENTS FROM REPORTS) *Let $R = (R_1, \dots, R_n)$ denote an elicited set of reported bundle-value pairs from each bidder obtained from MLCA (Algorithm 2) and let $R_{-i} := (R_1, \dots, R_{i-1}, R_{i+1}, \dots, R_n)$. We then calculate the VCG payments $p(R) = (p_1(R), \dots, p_n(R)) \in \mathbb{R}_+^n$ as follows:*

$$p_i(R) := \sum_{j \in N \setminus \{i\}} \hat{v}_j \left((a_{R_{-i}}^*)_j \right) - \sum_{j \in N \setminus \{i\}} \hat{v}_j \left((a_R^*)_j \right). \quad (19)$$

where $a_{R_{-i}}^*$ maximizes the reported social welfare when excluding bidder i , i.e.,

$$a_{R_{-i}}^* \in \operatorname{argmax}_{a \in \mathcal{F}} \widehat{V}(a | R_{-i}) = \operatorname{argmax}_{a \in \mathcal{F}} \sum_{\substack{j \in N \setminus \{i\}: \\ (a_j, \hat{v}_j(a_j)) \in R_j}} \hat{v}_j(a_j), \quad (20)$$

and a_R^* is a reported-social-welfare-maximizing allocation (including all bidders), i.e.,

$$a_R^* \in \operatorname{argmax}_{a \in \mathcal{F}} \widehat{V}(a | R) = \operatorname{argmax}_{a \in \mathcal{F}} \sum_{i \in N: (a_i, \hat{v}_i(a_i)) \in R_i} \hat{v}_i(a_i). \quad (21)$$

Therefore, when using VCG, bidder i ’s utility is:

$$u_i = v_i((a_R^*)_i) - p_i(R) \\ = v_i((a_R^*)_i) + \underbrace{\sum_{j \in N \setminus \{i\}} \hat{v}_j((a_R^*)_j)}_{\text{(a) Reported SW of main economy}} - \underbrace{\sum_{j \in N \setminus \{i\}} \hat{v}_j((a_{R_{-i}}^*)_j)}_{\text{(b) Reported SW of marginal economy}}.$$

Any beneficial misreport must increase the difference (a) – (b).

MLCA has two features that mitigate manipulations. First, MLCA explicitly queries each bidder’s marginal economy (Algorithm 2, Line 5), which implies that (b) is practically independent of bidder i ’s bid (Brero, Lubin, and Seuken (2021) provide experimental support for this). Second, MLCA enables bidders to “push” information to the auction which they deem useful. This mitigates certain manipulations that target (a), as it allows bidders to increase (a) with truthful information. Brero, Lubin, and Seuken (2021) argue that any remaining manipulation would be implausible as it would require almost complete information.

If we are willing to make two weak assumptions, we also obtain a theoretical incentive guarantee. Assumption 1 requires that, if all bidders bid truthfully, then MLCA finds an efficient allocation (we show in Appendix D.2 that in two of our domains: GSVM, LSVM, we indeed find the efficient allocation in the majority of cases). Assumption 2 requires that, for all bidders i , if all other bidders report truthfully, then the social welfare of bidder i ’s marginal economy is independent of his value reports. If both assumptions hold, then bidding truthfully is an ex-post Nash equilibrium in MLCA.

B Monotone-Value Neural Networks

In this Section, we provide proofs for all mathematical claims made in Section 3.1 *Theoretical Analysis and MIP-Formulation* (Appendix B.1, B.2 and B.3) and give an overview of bounds tightening via *interval arithmetic* for the MVNN-based MIP (Appendix B.4).

B.1 Proof of Lemma 1

Lemma 1. Let $\mathcal{N}_i^\theta : \mathcal{X} \rightarrow \mathbb{R}_+$ denote a MVNN from Definition 1. Then it holds that \mathcal{N}_i^θ fulfills (N) and (M), i.e. $\mathcal{N}_i^{(W^i, b^i)} \in \mathcal{V}$ for all $W^i \geq 0$ and $b^i \leq 0$.

Proof.

1. Monotonicity (M):

This property immediately follows, since (component wise) the weights $W^{i,k} \geq 0$ for all $k \in \{1, \dots, K_i\}$ and $\varphi_{0,t}(z)$ is monotonically increasing.

2. Normalization (N):

Since $\varphi_{0,t}(z) = 0$ for $z \leq 0$ and the biases fulfill (component wise) $b^{i,k} \leq 0$, we can conclude that $\mathcal{N}_i^\theta(\underbrace{(0, \dots, 0)}_{m\text{-times}}) = 0$.

□

B.2 Proof of Theorem 1

Theorem 1 (Universality). Any value function $\hat{v}_i : \mathcal{X} \rightarrow \mathbb{R}_+$ that satisfies (N) and (M) can be represented exactly as a MVNN \mathcal{N}_i^θ from Definition 1, i.e.,

$$\mathcal{V} = \left\{ \mathcal{N}_i^{(W^i, b^i)} : W^i \geq 0, b^i \leq 0 \right\}. \quad (22)$$

Proof.

$$1. \mathcal{V} \supseteq \left\{ \mathcal{N}_i^{(W^i, b^i)} : W^{i,k} \geq 0, b^{i,k} \leq 0 \forall k \in \{1, \dots, K_i\} \right\}$$

This direction follows immediately from Lemma 1.

$$2. \mathcal{V} \subseteq \left\{ \mathcal{N}_i^{(W^i, b^i)} : W^{i,k} \geq 0, b^{i,k} \leq 0 \forall k \in \{1, \dots, K_i\} \right\}$$

Let $(\hat{v}_i(x))_{x \in \mathcal{X}} \in \mathcal{V}$. For the reverse direction, we give a constructive proof, i.e., we construct a MVNN \mathcal{N}_i^θ with $\theta = (W_{\hat{v}_i}^i, b_{\hat{v}_i}^i)$ such that $\mathcal{N}_i^\theta(x) = \hat{v}_i(x)$ for all $x \in \mathcal{X}$.

Let $(w_j)_{j=1}^{2^m}$ denote the values corresponding to $(\hat{v}_i(x))_{x \in \mathcal{X}}$ sorted in increasing order, i.e. let $x_1 = (0, \dots, 0)$ with

$$w_1 := \hat{v}_i(x_1) = 0, \quad (23)$$

let $x_{2^m} = (1, \dots, 1)$ with

$$w_{2^m} := \hat{v}_i(x_{2^m}), \quad (24)$$

and $x_j, x_l \in \mathcal{X} \setminus \{x_1, x_{2^m}\}$ for $1 < l \leq j \leq 2^m - 1$ with

$$w_j := \hat{v}_i(x_j) \leq w_l := \hat{v}_i(x_l). \quad (25)$$

In the following, we slightly abuse the notation and write for $x_l, x_j \in \mathcal{X}$ $x_l \subseteq x_j$ iff for the corresponding sets $A_j, A_l \in 2^M$ it holds that $A_j \subseteq A_l$. Furthermore, we denote by $\langle \cdot, \cdot \rangle$ the Euclidean scalar product on \mathbb{R}^m . Then, for all $x \in \mathcal{X}$:

$$\begin{aligned} \hat{v}_i(x) &= \sum_{l=1}^{2^m-1} (w_{l+1} - w_l) \mathbb{1}_{\{\forall j \in \{1, \dots, l\} : x \not\subseteq x_j\}} \\ &= \sum_{l=1}^{2^m-1} (w_{l+1} - w_l) \varphi_{0,1} \left(\sum_{j=1}^l \varphi_{0,1}(\langle 1 - x_j, x \rangle) - (l-1) \right), \end{aligned} \quad (26)$$

where the second equality follows since

$$x \not\subseteq x_j \iff \langle 1 - x_j, x \rangle \geq 1 \quad (28)$$

$$\iff \varphi_{0,1}(\langle 1 - x_j, x \rangle) = 1, \quad (29)$$

which implies that

$$\forall j \in \{1, \dots, l\} : x \not\subseteq x_j \iff \sum_{j=1}^l \varphi_{0,1}(\langle 1 - x_j, x \rangle) = l, \quad (30)$$

and

$$\mathbb{1}_{\{\forall j \in \{1, \dots, l\} : x \not\subseteq x_j\}} = \varphi_{0,1} \left(\sum_{j=1}^l \varphi_{0,1}(\langle 1 - x_j, x \rangle) - (l-1) \right) \quad (31)$$

Finally, Equation (27) can be equivalently written in matrix notation as

$$\underbrace{\begin{bmatrix} w_2 - w_1 \\ w_3 - w_2 \\ \vdots \\ w_{2^m} - w_{2^m-1} \end{bmatrix}}_{(W_{\hat{v}_i}^{i,3})^T \in \mathbb{R}_{\geq 0}^{2^m-1}} \varphi_{0,1} \left(W_{\hat{v}_i}^{i,2} \varphi_{0,1} \left(\underbrace{\begin{bmatrix} 1 - x_1 \\ 1 - x_2 \\ \vdots \\ 1 - x_{2^m-1} \end{bmatrix}}_{W_{\hat{v}_i}^{i,1} \in \mathbb{R}_{\geq 0}^{(2^m-1) \times m}} x \right) + \underbrace{\begin{bmatrix} 0 \\ -1 \\ \vdots \\ -(2^m-2) \end{bmatrix}}_{b_{\hat{v}_i}^{i,2} \in \mathbb{R}_{\leq 0}^{2^m-1}} \right)$$

with $W_{\hat{v}_i}^{i,2} \in \mathbb{R}_{\geq 0}^{(2^m-1) \times (2^m-1)}$ a lower triangular matrix of ones, i.e.,

$$W_{\hat{v}_i}^{i,2} := \begin{bmatrix} 1 & 0 & \dots & 0 \\ \vdots & \ddots & \ddots & \vdots \\ \vdots & & \ddots & 0 \\ 1 & \dots & \dots & 1 \end{bmatrix}.$$

From that, we can see that the last term is indeed a MVNN $\mathcal{N}_i^\theta(x) = W_{\hat{v}_i}^{i,3} \varphi_{0,1} \left(W_{\hat{v}_i}^{i,2} \varphi_{0,1} \left(W_{\hat{v}_i}^{i,1} x + b_{\hat{v}_i}^{i,1} \right) \right)$ with four layers in total (i.e., two hidden layers) and respective dimensions $[m, 2^m - 1, 2^m - 1, 1]$.

□

B.3 Proof of Lemma 2

Lemma 2. Fix bidder $i \in N$, let $k \in \{2, \dots, K_i - 1\}$ and denote the pre-activated output of the k^{th} hidden layer as $o^{i,k} := W^{i,k-1} z^{i,k-1} + b^{i,k-1}$ with $W^{i,k-1} \in \mathbb{R}^{d_k \times d_{k-1}}, b^{i,k-1} \in \mathbb{R}^{d_k}$. Then the value of the k^{th} hidden layer $z^{i,k} := \varphi(o^{i,k}) = \min(1, \max(0, o^{i,k})) = -\max(-1, -\eta^{i,k})$, with $\eta^{i,k} := \max(0, o^{i,k})$ can be equivalently expressed by the following linear constraints:

$$o^{i,k} \leq \eta^{i,k} \leq o^{i,k} + y^{i,k} \cdot L_1^{i,k} \quad (32)$$

$$0 \leq \eta^{i,k} \leq (1 - y^{i,k}) \cdot L_2^{i,k} \quad (33)$$

$$\eta^{i,k} - \mu^{i,k} \cdot L_3^{i,k} \leq z^{i,k} \leq \eta^{i,k} \quad (34)$$

$$1 - (1 - \mu^{i,k}) \cdot L_4^{i,k} \leq z^{i,k} \leq 1 \quad (35)$$

$$y^{i,k} \in \{0, 1\}^{d_k}, \quad \mu^{i,k} \in \{0, 1\}^{d_k}, \quad (36)$$

where $L_1^{i,k}, L_2^{i,k}, L_3^{i,k}, L_4^{i,k} \in \mathbb{R}_+$ are large enough constants for the respective big-M constraints.

Proof. For all $j \in \{1, \dots, d_k^i\}$ we distinguish the following three cases:

Case 1: $o_j^{i,k} \in (-\infty, 0] \Rightarrow \varphi(o_j^{i,k})_j = 0$

(i) & (ii) $\Rightarrow y_j^{i,k} = 1 \Rightarrow \eta_j^{i,k} = 0$

(iii) & (iv) $\Rightarrow \mu_j^{i,k} = 0 \Rightarrow z_j^{i,k} = \eta_j^{i,k} = 0$

Case 2: $o_j^{i,k} \in (0, 1] \Rightarrow \varphi(o_j^{i,k})_j = o_j^{i,k}$

(i) & (ii) $\Rightarrow y_j^{i,k} = 0 \Rightarrow \eta_j^{i,k} = o_j^{i,k}$

(iii) & (iv) $\Rightarrow \mu_j^{i,k} = 0 \Rightarrow z_j^{i,k} = \eta_j^{i,k} = o_j^{i,k}$

Case 3: $o_j^{i,k} \in (1, +\infty] \Rightarrow \varphi(o_j^{i,k})_j = 1$

(i) & (ii) $\Rightarrow y_j^{i,k} = 0 \Rightarrow \eta_j^{i,k} = o_j^{i,k}$

(iii) & (iv) $\Rightarrow \mu_j^{i,k} = 1 \Rightarrow z_j^{i,k} = 1$

Thus, in total $z^{i,k} = \varphi(o^{i,k})$. □

B.4 Interval Arithmetic Bounds Tightening for MVNNs

In this Section, we consider a bReLU $\varphi_{0,t}$ with cutoff $t > 0$ and mark it in red. This helps when implementing the MIP, i.e. it particularly shows more clearly where the cutoff t propagates in the respective equations. First, we recall Lemma 1 for a general cutoff t , where for the sake of readability we remove the bidder index $i \in N$ from all variables.

Lemma 2. Let $k \in \{2, \dots, K-1\}$ and let the pre-activated output of the k^{th} hidden layer be given as $W^{k-1} z^{k-1} + b^{k-1}$ with $W^{k-1} \in \mathbb{R}^{d_k \times d_{k-1}}, b^{k-1} \in \mathbb{R}^{d_k}$. Then the value of the k^{th} hidden layer $z^k := \varphi_{0,t}(W^{k-1} z^{k-1} + b^{k-1}) = \min(\textcolor{red}{t}, \max(0, (W^{k-1} z^{k-1} + b^{k-1}))) = -\max(-\textcolor{red}{t}, -\eta^k)$, with $\eta^k := \max(0, W^{k-1} z^{k-1} + b^{k-1})$ can be equivalently expressed by the following linear constraints:

$$W^{k-1} z^{k-1} + b^{k-1} \leq \eta^k \leq W^{k-1} z^{k-1} + b^{k-1} + y^k L_1^k \quad (37)$$

$$0 \leq \eta^k \leq (1 - y^k) L_2^k \quad (38)$$

$$\eta^k - \mu^k L_3^k \leq z^k \leq \eta^k \quad (39)$$

$$\textcolor{red}{t} - (1 - \mu^k) L_4^k \leq z^k \leq \textcolor{red}{t} \quad (40)$$

where $y^k \in \{0, 1\}^{d_k}, \mu^k \in \{0, 1\}^{d_k}$, and $L_1^k, L_2^k, L_3^k, L_4^k \in \mathbb{R}_+$ are large enough constants for the respective big-M constraints.

Interval Arithmetic (IA) for Single Neurons For any $k \in \{2, \dots, K-1\}$ let $W^{k-1} \geq 0$ and $b^{k-1} \leq 0$ be the weights of its affine linear transformation. Furthermore, let z^{k-1} be the output of the previous layer. and, let

$$z^k = \varphi_{0,t}(W^{k-1} z^{k-1} + b^{k-1}) \quad (41)$$

be the output of the current layer.

Given already computed IA bounds for z_i^{k-1} , i.e., $[L(z_i^{k-1}), U(z_i^{k-1})] \subseteq [0, \textcolor{red}{t}]$, we can then calculate the IA bounds $L(z_l^k), U(z_l^k)$ for z_l^k such that

$$z^k \in \prod_{l=1}^{d^k} [L(z_l^k), U(z_l^k)] \quad (42)$$

as follows:

1. Upper bound (pre-activated):

$$U^{\text{pre}}(z^k) = \quad (43)$$

$$= \max_{z^{k-1} \in \prod_{l=1}^{d^{k-1}} [L(z_l^{k-1}), U(z_l^{k-1})]} \left\{ W^{k-1} z^{k-1} + b^{k-1} \right\} \quad (44)$$

$$= \left(\sum_l W_{j,l}^{k-1} \cdot U(z_l^{k-1}) \right)_{j=1}^{d^k} + b^{k-1} \quad (45)$$

2. Upper bound:

$$U(z^k) = \varphi_{0,t}(U^{\text{pre}}(z^k)) \quad (46)$$

3. Lower bound (pre-activated):

$$L^{\text{pre}}(z^k) = \quad (47)$$

$$= \min_{z^{k-1} \in \prod_{l=1}^{d^{k-1}} [L(z_l^{k-1}), U(z_l^{k-1})]} \left\{ W^{k-1} z^{k-1} + b^{k-1} \right\} \quad (48)$$

$$= \left(\sum_l W_{j,l}^{k-1} \cdot L(z_l^{k-1}) \right)_{j=1}^{d^k} + b^{k-1} \quad (49)$$

Note, that the preactivated lower bound $L^{\text{pre}}(z^k)$ is always non-positive, i.e. $L^{\text{pre}}(z^k) \leq 0$. This can be seen as follows: start with a $L(z^1) = \mathbf{0}_m$ (per definition where $m =: d^1$ denotes the number of items). Then since all biases are non-positive $L^{\text{pre}}(z^2) \leq 0 \implies L(z^2) = \mathbf{0}_{d^2}$, and so forth. Thus, we get for the lower bounds:

4. Lower bound:

$$L(z^k) = \varphi_{0,t}(L^{\text{pre}}(z^k)) = \mathbf{0}_{d^k} \quad (50)$$

Removing Constraints with IA In the following cases, we can remove the constraints and corresponding variables in Lemma 2:

1. Case:

If $U^{\text{pre}}(z_l^k) \leq 0 \implies z_l^k = 0$ and one can remove the l^{th} components from all constraints (37) – (40) and the corresponding variables for layer k .

2. Case:

If $L^{\text{pre}}(z_l^k) \in [0, t]$ and $U^{\text{pre}}(z_l^k) \in (0, t] \implies z_l^k = (W^{k-1} z^{k-1} + b^{k-1})_l$ and one can remove the l^{th} components from all constraints (37) – (40) and the corresponding variables for layer k .

3. Case:

If $L^{\text{pre}}(z_l^k) = 0$ and $U^{\text{pre}}(z_l^k) > t \implies \eta_l^k = (W^{k-1} z^{k-1} + b^{k-1})_l$ and one can remove the l^{th} components from all constraints (37) – (38) and the corresponding variables for layer k .

4. Case:

If $L^{\text{pre}}(z_l^k) < 0$ and $U^{\text{pre}}(z_l^k) \in (0, t] \implies z_l^k = \eta_l^k$ and one can remove the l^{th} components from all constraints (39) – (40) and the corresponding variables for layer k .⁵

Interval Arithmetic for the Four Big-M Constraints

Recall, that $L(z^k) = \mathbf{0}_{d^k}$ for all $k \in \{1, \dots, K-1\}$. Let $m =: d^1$ denote the number of items to be allocated.

We present standard IA bounds where one starts for $z^1 \in \{0, 1\}^m$ with $L(z^1) = \mathbf{0}_m$ and $U(z^1) = \mathbf{1}_m$ (per definition) and iteratively for $k \in \{3, \dots, K-1\}$ propagates through the network for given bounds on z^{k-1} , i.e., $z^{k-1} \in \mathcal{Z}^{k-1} := \prod_{l=1}^{d^{k-1}} [0, U(z_l^{k-1})] \subset [0, t]^{d^{k-1}}$.

1. L_1^k only appears when $y^k = 1$, which implies that $\eta^k = 0$ and $W^{k-1} z^{k-1} + b^{k-1} \leq 0$. Thus, Equation (37) implies that $L_1^k + \min_{z^{k-1} \in \mathcal{Z}^{k-1}} \{W^{k-1} z^{k-1} + b^{k-1}\} \geq 0$ and we get

$$L_1^k = \max \left\{ 0, - \min_{z^{k-1} \in \mathcal{Z}^{k-1}} \{W^{k-1} z^{k-1} + b^{k-1}\} \right\} \quad (51)$$

$$= \max \left\{ 0, \left(\sum_{l: W_{j,l}^{k-1} < 0} |W_{j,l}^{k-1}| \cdot U(z_l^{k-1}) \right) - b^{k-1} \right\}_{j=1}^{d^k} \quad (52)$$

$$= \max \{0, -b^{k-1}\} \quad (53)$$

where the last equality follows since per definition any MVNN only has positive weights.

2. L_2^k only appears when $y^k = 0$ which implies that $\eta^k = W^{k-1} z^{k-1} + b^{k-1} \geq 0$. Thus, Equation (38) implies that $L_2^k \geq \eta^k = W^{k-1} z^{k-1} + b^{k-1}$ and we get

$$L_2^k = \max_{z^{k-1} \in \mathcal{Z}^{k-1}} \{W^{k-1} z^{k-1} + b^{k-1}\} \quad (54)$$

$$= \max \left\{ 0, \left(\sum_{l: W_{j,l}^{k-1} > 0} W_{j,l}^{k-1} \cdot U(z_l^{k-1}) \right) + b^{k-1} \right\}_{j=1}^{d^k} \quad (55)$$

$$= \max \left\{ 0, \left(\sum_l W_{j,l}^{k-1} \cdot U(z_l^{k-1}) \right) + b^{k-1} \right\}_{j=1}^{d^k}, \quad (56)$$

where the last equality follows since per definition any MVNN only has positive weights.

3. L_3^k only appears when $\mu^k = 1$ which implies that $z^k = t$ and $\eta^k = W^{k-1} z^{k-1} + b^{k-1} \geq t$. Thus, Equation (39) implies that $t = z^k \geq \eta^k - L_3^k \iff L_3^k \geq \eta^k - t \iff L_3^k \geq W^{k-1} z^{k-1} + b^{k-1} - t$ and we get

$$L_3^k = \max_{z^{k-1} \in \mathcal{Z}^{k-1}} \{W^{k-1} z^{k-1} + b^{k-1} - t\} \quad (57)$$

$$= \max \{0, L_2^k - t\} \quad (58)$$

4. For L_4^k only appears when $\mu^k = 0$. In this case, we get from Equation (40) that $t - L^4 \leq z^k$ and we get

$$L^4 = \max_{z^k \in \mathcal{Z}^k} \{t - z^k\} = t \quad (59)$$

B.5 Implementation Details - MVNNs

All MVNNs were implemented in PyTorch (Paszke et al. 2019) and differ in the ways they enforce element-wise non-negative weights and element-wise non-positive biases. Additionally to the MVNN-RELU-PROJECTED version (discussed in the main paper), we considered the following MVNN-implementations:

MVNN-ABS and MVNN-RELU For this method, we add an additional node to the computational graph and element-wisely transform the weights W^i via the absolute value $z \mapsto |z|$ or ReLU $z \mapsto \max(0, z)$ to ensure non-negativity. For the biases b^i we analogously use $z \mapsto -|z|$

⁵In all experiments presented in this paper, we have not taken advantage of Case 3 and 4. We believe that we can further improve the computational performance of MVNN by incorporating these cases too.

Hyperparameters	Type	Range	Scale
Optimizer	Categorical	[Adam, SGD]	
Batch Size	Integer	[1, 4]	
Num. Hidden Layers	Integer	[1, 3]	
Total Num. Neurons	Integer	[1, 64]	
L2	Float	[1e-10, 1e-6]	log
Learning Rate	Float	[1e-4, 1e-2]	log
Epochs	Integer	[50, 400]	
Loss Function	Categorical	[MSE, MAE]	

Table 4: HPO space used in SMAC.

or $z \mapsto -\max(0, -z)$ to ensure non-positivity. Importantly, we *differentiate* through $z \mapsto \pm|z|$ or $z \mapsto \pm \max(0, \pm z)$ in every gradient descent (GD) step. We refer to these implementation variants as MVNN-ABS and MVNN-RELU. After the last GD step we apply *post-processing* and project W^i and b^i again via $z \mapsto \pm|z|$ and $z \mapsto \pm \max(0, \pm z)$.

MVNN-ABS-PROJECTED We do not consider a MVNN-ABS-PROJECTED implementation, since one can prove that in the classic GD algorithm this version is mathematically equivalent to MVNN-ABS.

C Details Prediction Performance

C.1 Data Generation - Prediction Performance

Train/Val/Test-Split For every domain, bidder type and considered amount of training data T we create the data in the following way: For each seed we let SATS create a value function and uniformly at random select T different bundles from the bidder-specific-feasible (using the SATS method *get_uniform_random_bids*) bundle space \mathcal{X} (training set). We measure the metrics of a method trained on the training data of a seed based on randomly selected different bundles from the same bundle space \mathcal{X} (approx. 52 000 for the HPO seeds (validation set) and approx. 210 000 for the test seeds (test set)). We use HPO seeds 0-20 only for the HPO (validation sets) and test seeds 21-50 only for reporting the values in this paper (test sets).

C.2 HPO - Prediction Performance

Table 4 shows the hyperparameter ranges from our HPO. Cosine Annealing (Loshchilov and Hutter 2017) was used to decay the learning to zero within the number of training epochs. Occasionally, the neural networks (both MVNNs and plain NNs) diverged during training (determined if $r_{xy} < 0.9$ on train set) hence we added 20 retries to the training to make sure that we obtain a valid network.

Experimentally, we found that MVNNs need the training data to be normalized to be within $[0, 1]$, as a result of the bReLU activation functions bounded output. On the other hand, Plain NNs worked better if the data was normalized to be within $[0, 500]$ for all considered SATS domains.

The computational budget of the HPO was 12 hours. All experiments were conducted on a compute cluster running Debian GNU/Linux 10 (buster) with Intel Xeon E5-2650 v4 2.20GHz processors with 48 logical cores and 128GB RAM and Intel E5 v2 2.80GHz processors with 40 logical cores and 128GB RAM and Python 3.7.10.

C.3 Detailed Results - Prediction Performance

Table 7 shows the detailed prediction performance results including all optimized hyperparameters for the MVNN-ABS and the MVNN-RELU-PROJECTED implementation of MVNNs. The MVNN-RELU implementation led to similar results as the MVNN-RELU-PROJECTED implementation, and therefore we do not present them in this table.

In Table 8, we visualize for all other SATS domains the prediction performance capabilities of MVNNs vs plain NNs. Overall, Table 7 and 8 show that MVNNs have a superior generalization performance across all SATS domains and bidder types.

D Details MVNN-based Iterative CA

D.1 Details Experimental Setup - MVNN-based Iterative CA

We used 50 auction instances for evaluation with seeds (for generating the SATS instances) 10001-10050 which do not intersect with the seeds used in Section C.1 for prediction performance. All experiments were conducted on the same compute cluster as in Appendix C.2.

Note, that we add the empty bundle to the initial elicited bundles Q_{init} , as we know its value to be 0 a priori. This has no impact for MVNNs as they estimate empty bundles to have zero value by definition but adds extra information for plain NNs.

For all SATS domains we specified a minimum relative gap of 1e-2 and a timeout of 300s.

D.2 Detailed Results - MVNN-based Iterative CA

In Table 5 we present detailed results of MLCA with MVNNs vs MLCA with plain NNs. The revenue and runtime should be considered with care. The revenue is influenced by our choice to use early stopping whenever we already found an efficient allocation at an intermediary iteration as discussed in the main paper. The shown runtime is not comparable between MVNNs and NNs as they do not use the same architecture, but the one found during HPO. See Section 5.3 in the main paper for a fair runtime comparison.

For the presentation in the main paper (i.e., Table 3 in the main paper), we selected the best MVNN and plain NN per domain, i.e. the ones marked with a star. In Figures 5, 6, 7 and 8 we present a detailed boxplot version of the efficiency loss path plots for the best model per domain.

D.3 Detailed Revenue Analysis - MVNN-based Iterative CA

Recall the VCG-payments from Definition 2, i.e., for a set of elicited reports R bidder i 's VCG-payment is given as:

$$p_i(R) := \underbrace{\sum_{j \in N \setminus \{i\}} \hat{v}_j \left((a_{R-i}^*)_j \right)}_{=: \text{Marg}_{-i}} - \underbrace{\sum_{j \in N \setminus \{i\}} \hat{v}_j \left((a_R^*)_j \right)}_{=: \text{Main}_{-i}},$$

DOMAIN	T	Q_{INIT}	Q_{ROUND}	Q_{MAX}	EFFICIENCY LOSS IN % ↓		REVENUE IN % ↑		RUNTIME IN HRS.	
					MVNN	NN	MVNN	NN	MVNN	NN
GSVM	10	40	4	100	00.00 ± 0.00	00.01 ± 0.02	60.11 ± 3.86	58.59 ± 4.35	00.14 ± 0.03	00.15 ± 0.05
	20	40	4	100	00.00 ± 0.00	*00.00 ± 0.00	59.07 ± 3.84	55.71 ± 4.46	00.08 ± 0.01	00.06 ± 0.01
	50	40	4	100	*00.00 ± 0.00	00.00 ± 0.00	52.77 ± 5.04	56.09 ± 4.57	00.06 ± 0.01	00.07 ± 0.01
LSVM	10	40	4	100	01.63 ± 0.75	03.19 ± 01.59	70.14 ± 4.23	65.23 ± 3.83	00.93 ± 0.36	01.16 ± 0.23
	50	40	4	100	*00.70 ± 0.40	03.11 ± 01.52	70.70 ± 4.63	64.07 ± 4.24	00.54 ± 0.15	01.28 ± 0.32
	100	40	4	100	01.27 ± 0.55	*02.91 ± 01.44	71.09 ± 4.35	65.10 ± 3.90	00.52 ± 0.12	00.44 ± 0.10
SRVM	10	40	4	100	00.67 ± 0.10	01.27 ± 0.23	50.86 ± 2.31	46.93 ± 2.07	01.86 ± 0.10	01.59 ± 0.09
	50	40	4	100	00.49 ± 0.07	01.15 ± 0.31	50.70 ± 2.44	45.59 ± 2.72	20.72 ± 0.52	02.17 ± 0.21
	100	40	4	100	*00.23 ± 0.06	*01.13 ± 0.22	51.18 ± 2.52	46.30 ± 2.87	20.12 ± 1.77	00.68 ± 0.06
MRVM	10	40	4	100	*08.16 ± 0.41	10.96 ± 0.76	34.45 ± 2.06	41.68 ± 1.34	02.59 ± 0.13	06.08 ± 0.40
	100	40	4	100	08.67 ± 0.43	10.19 ± 0.89	35.04 ± 1.91	41.91 ± 1.39	01.96 ± 0.12	03.33 ± 0.37
	300	40	4	100	09.96 ± 0.49	*09.05 ± 0.53	32.72 ± 2.17	39.66 ± 1.20	00.96 ± 0.04	01.84 ± 0.24

Table 5: Efficiency loss, relative revenue and runtime of MLCA with MVNNs vs MLCA with plain NNs. Shown are averages including a 95% CI on a test set of 50 auction instances in all four SATS domains. The best MVNN and plain NN per domain based on the lowest efficiency loss are marked with a star (if the final efficiency loss is the same for multiple incumbents we selected the incumbent that reached 0% with the fewest number of queries).

DOMAIN	T	NUMBER OF QUERIES			AVG. MARG. SCWS (%)			AVG. MAIN SCWS (%)			REVENUE IN % ↑		
		MVNN	NN	RS	MVNN	NN	RS	MVNN	NN	RS	MVNN	NN	RS
GSVM	10	59.1	52.6	100.0	94.31	94.09	67.05	85.71	85.71	59.90	60.11 ± 3.86	58.59 ± 4.35	52.19 ± 2.39
	20	54.3	47.8	100.0	94.16	93.69	67.05	85.71	85.71	59.90	59.07 ± 3.84	55.71 ± 4.46	52.19 ± 2.39
	50	47.2	48.3	100.0	93.25	93.74	67.05	85.71	85.71	59.90	52.77 ± 5.04	56.09 ± 4.57	52.19 ± 2.39
LSVM	10	74.2	75.5	100.0	93.58	91.41	64.57	81.95	80.62	55.67	70.14 ± 4.23	65.23 ± 3.83	53.58 ± 1.84
	50	68.6	73.2	100.0	94.48	91.28	64.57	82.74	80.69	55.67	70.70 ± 4.63	64.07 ± 4.24	53.58 ± 1.84
	100	73.2	73.0	100.0	94.04	91.63	64.57	82.26	80.86	55.67	71.09 ± 4.35	65.10 ± 3.90	53.58 ± 1.84
SRVM	10	100.0	100.0	100.0	92.53	91.34	69.43	85.13	84.62	62.12	50.86 ± 2.31	46.93 ± 2.07	51.56 ± 2.07
	50	99.4	99.9	100.0	92.66	91.35	69.43	85.29	84.72	62.12	50.70 ± 2.44	45.59 ± 2.72	51.56 ± 2.07
	100	98.9	99.8	100.0	92.98	91.47	69.43	85.52	84.74	62.12	51.18 ± 2.52	46.30 ± 2.87	51.56 ± 2.07
MRVM	10	100.0	100.0	100.0	86.12	84.39	50.39	82.68	80.22	46.03	34.45 ± 2.06	41.68 ± 1.34	43.58 ± 0.65
	100	100.0	100.0	100.0	85.70	85.04	50.39	82.22	80.83	46.03	35.04 ± 1.91	41.91 ± 1.39	43.58 ± 0.65
	300	100.0	100.0	100.0	84.29	85.86	50.39	81.03	81.87	46.03	32.72 ± 2.17	39.66 ± 1.20	43.58 ± 0.65

Table 6: Normalized average social welfare in the marginal economies and main economies when excluding one bidder for MVNNs, NNs and random search (RS). Additionally, we print the average number of queries, that can differ between MVNN and NN incumbents due to early termination of MLCA. Shown are averages over the same test set of 50 auction instances as in Table 5.

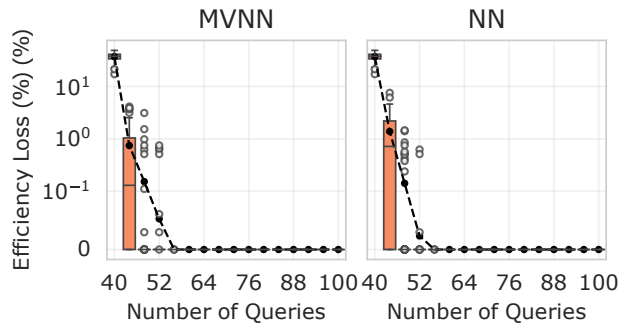


Figure 5: Efficiency loss path of MVNN vs plain NN in GSVM with the corresponding best MVNN ($T = 50$) and plain NN ($T = 20$) from Table 5. Averages are shown as black dots. We use a semi-logarithmic scale with linear range $[0, 1e-2]$.

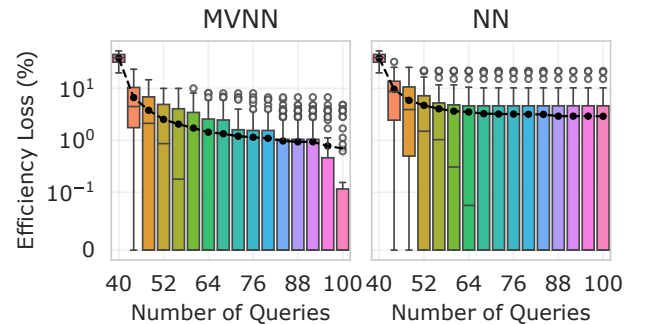


Figure 6: Efficiency loss path of MVNN vs plain NN in LSVM with the corresponding best MVNN ($T = 50$) and plain NN ($T = 100$) from Table 5. Averages are shown as black dots. We use a semi-logarithmic scale with linear range $[0, 1e-1]$.

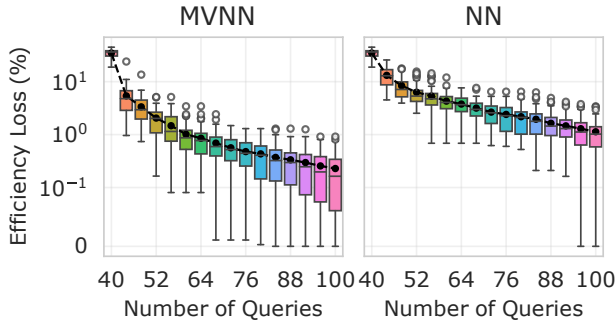


Figure 7: Efficiency loss path of MVNN vs plain NN in SRVM with the corresponding best MVNN ($T = 100$) and best plain NN ($T = 100$) from Table 5. Averages are shown as black dots. We use a semi-logarithmic scale with linear range $[0, 1e-1]$.

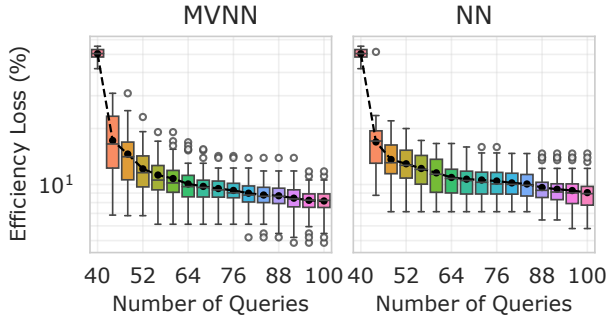


Figure 8: Efficiency loss path of MVNN vs plain NN in MRVM with the corresponding best MVNN ($T = 10$) and plain NN ($T = 300$) from Table 5. Averages are shown as black dots. Only logarithmic scale.

where Marg_{-i} is for a given set of reports R the optimal social welfare (SCW) in the *marginal* economy when excluding bidder $i \in N$ and Main_{-i} denotes the SCW of the *main* economy when excluding bidder i . The larger the differences $\text{Marg}_{-i} - \text{Main}_{-i}$, $i \in N$ the more revenue is generated in the auction. In Table 6, we print the normalized average marginal SCW ($\frac{1}{n} \sum_{i \in N} \text{Marg}_{-i} / V(a^*)$) (**AVG. MARG. SCWs (%)**) and the normalized average main SCW when excluding one bidder ($\frac{1}{n} \sum_{i \in N} \text{Main}_{-i} / V(a^*)$) (**AVG. MAIN SCWs (%)**) averaged over the 50 auction instances corresponding to Table 5. Using this notation, the average total relative revenue of the auction is then the difference of the normalized average marginal SCW and the normalized average main SCW when excluding one bidder times the number of bidders, i.e.,

$$n \left(\left(\frac{1}{n} \sum_{i \in N} \text{Marg}_{-i} \right) / V(a^*) - \left(\frac{1}{n} \sum_{i \in N} \text{Main}_{-i} \right) / V(a^*) \right).$$

Recall, that we terminate MLCA in an intermediate iteration, if it already found an efficient allocation (to save computational costs), i.e., incurred no efficiency loss. Due to this early termination the revenue can be worse off since fewer bundles are elicited in the marginal economies. If one runs a

full auction without early termination, the revenue can only improve after the efficient allocation was already found (because Main_{-i} can not increase anymore after the efficient allocation was already found, but Marg_{-i} can still improve).

In Table 6, we present a detailed revenue analysis for all domains. Table 6 shows that overall the MVNN's achieved (normalized) SCWs are larger both in the marginal economies as well as in the main economies when excluding one bidder.

In GSVM, we find the efficient allocation very early (see Figure 5 or Table 6), so the revenue is mainly determined by the number of queries. Without early determination, 60% revenue should be easily achievable for MVNNs. For LSVM and SRVM, we see that even with less queries MVNNs can outperform plain NNs consistently in terms of revenue. Without early termination, we expect this margin to be even higher (because this would add more queries for MVNNs).

In MRVM, we see that the best MVNN ($T = 10$) achieves an average difference of $86.12 - 82.68 = 3.44$ while the best plain NN ($T=300$) achieves an average difference of $85.86 - 81.87 = 3.98$. This implies the larger revenue ($\approx 5\% = 10 \cdot 0.5\%$) of plain NNs in MRVM from Table 3 in the main paper. A possible explanation for the larger revenue of plain NNs in MRVM is that, with each query MVNNs much more exploit the economy for that we solve the WDP, while plain NNs are more random and thus the query that solves the WDP for the main economy is not perfectly specialized for the main economy, but only slightly more helpful for the main economy than for the other economies. Recall that MLCA asks in each iteration each bidder Q^{round}_{-} many queries: one main economy query and $Q^{\text{round}}_{-} - 1$ marginal economy queries. Thus, if $Q^{\text{round}} < n$, MLCA generates more queries for the main economy than for each marginal economy and MVNNs improve the main economy even more than they improve the marginal economies, since their queries are highly specialized and exploiting. This effect is the strongest for MRVM as it has the largest ratio of the number of bidders n and Q^{round} .

However, if the objective would be to maximize revenue rather than efficiency, MVNNs could achieve as good or better revenue than plain NNs when we set $Q^{\text{round}} = n$, since then both main and marginal economies would be equally improved by the advantages of MVNNs (again with $Q^{\text{round}} = 4$ the main economy profits more from the advantages of the MVNNs than the marginal economies see Table 6).

As expected, for random search (RS) the (normalized) SCWs in both the marginal economies and the main economies when excluding one bidder are much lower compared to MVNNs and NNs. However, since *each* economies' SCW is bad, their differences and thus the revenue does not have to be worse. Moreover, since RS treats all economies equally and particularly is not specialized towards the main economies (in contrast to MVNN-MLCA or NN-MLCA with $Q^{\text{round}} < n$), RS's revenue can be even higher compared to MVNNs and NNs (e.g. in SRVM and MRVM).

Domain	T Bidder	T _{xy}				KT				MAE				Architecture				Batch Size				L2-Reg.				Optimizer				Learning Rate				Loss				Epochs																																																																																																																																																																																																																																																																																																																																																																																																																																																																																																																																																																																																																																																																																																																																																																																																																																																																																																																										
		NN		MVNN		MVNN		RELU-Proj.		NN		MVNN		MVNN		RELU-Proj.		NN		MVNN		MVNN		RELU-Proj.		NN		MVNN		MVNN		RELU-Proj.		NN		MVNN		MVNN		RELU-Proj.		Plain		Abs		Plain		Abs																																																																																																																																																																																																																																																																																																																																																																																																																																																																																																																																																																																																																																																																																																																																																																																																																																																																																																																
		Plain	Abs	Plain	Abs	Plain	Abs	Plain	Abs	Plain	Abs	Plain	Abs	Plain	Abs	Plain	Abs	Plain	Abs	Plain	Abs	Plain	Abs	Plain	Abs	Plain	Abs	Plain	Abs	Plain	Abs	Plain	Abs	Plain	Abs	Plain	Abs	Plain	Abs	Plain	Abs	Plain	Abs	Plain	Abs	Plain	Abs	Plain	Abs	Plain	Abs	Plain	Abs	Plain	Abs	Plain	Abs	Plain	Abs	Plain	Abs	Plain	Abs	Plain	Abs	Plain	Abs	Plain	Abs	Plain	Abs	Plain	Abs	Plain	Abs	Plain	Abs	Plain	Abs	Plain	Abs	Plain	Abs	Plain	Abs	Plain	Abs	Plain	Abs	Plain	Abs	Plain	Abs	Plain	Abs	Plain	Abs	Plain	Abs	Plain	Abs	Plain	Abs	Plain	Abs	Plain	Abs	Plain	Abs	Plain	Abs	Plain	Abs	Plain	Abs	Plain	Abs	Plain	Abs	Plain	Abs	Plain	Abs	Plain	Abs	Plain	Abs	Plain	Abs	Plain	Abs	Plain	Abs	Plain	Abs	Plain	Abs	Plain	Abs	Plain	Abs	Plain	Abs	Plain	Abs	Plain	Abs	Plain	Abs	Plain	Abs	Plain	Abs	Plain	Abs	Plain	Abs	Plain	Abs	Plain	Abs	Plain	Abs	Plain	Abs	Plain	Abs	Plain	Abs	Plain	Abs	Plain	Abs	Plain	Abs	Plain	Abs	Plain	Abs	Plain	Abs	Plain	Abs	Plain	Abs	Plain	Abs	Plain	Abs	Plain	Abs	Plain	Abs	Plain	Abs	Plain	Abs	Plain	Abs	Plain	Abs	Plain	Abs	Plain	Abs	Plain	Abs	Plain	Abs	Plain	Abs	Plain	Abs	Plain	Abs	Plain	Abs	Plain	Abs	Plain	Abs	Plain	Abs	Plain	Abs	Plain	Abs	Plain	Abs	Plain	Abs	Plain	Abs	Plain	Abs	Plain	Abs	Plain	Abs	Plain	Abs	Plain	Abs	Plain	Abs	Plain	Abs	Plain	Abs	Plain	Abs	Plain	Abs	Plain	Abs	Plain	Abs	Plain	Abs	Plain	Abs	Plain	Abs	Plain	Abs	Plain	Abs	Plain	Abs	Plain	Abs	Plain	Abs	Plain	Abs	Plain	Abs	Plain	Abs	Plain	Abs	Plain	Abs	Plain	Abs	Plain	Abs	Plain	Abs	Plain	Abs	Plain	Abs	Plain	Abs	Plain	Abs	Plain	Abs	Plain	Abs	Plain	Abs	Plain	Abs	Plain	Abs	Plain	Abs	Plain	Abs	Plain	Abs	Plain	Abs	Plain	Abs	Plain	Abs	Plain	Abs	Plain	Abs	Plain	Abs	Plain	Abs	Plain	Abs	Plain	Abs	Plain	Abs	Plain	Abs	Plain	Abs	Plain	Abs	Plain	Abs	Plain	Abs	Plain	Abs	Plain	Abs	Plain	Abs	Plain	Abs	Plain	Abs	Plain	Abs	Plain	Abs	Plain	Abs	Plain	Abs	Plain	Abs	Plain	Abs	Plain	Abs	Plain	Abs	Plain	Abs	Plain	Abs	Plain	Abs	Plain	Abs	Plain	Abs	Plain	Abs	Plain	Abs	Plain	Abs	Plain	Abs	Plain	Abs	Plain	Abs	Plain	Abs	Plain	Abs	Plain	Abs	Plain	Abs	Plain	Abs	Plain	Abs	Plain	Abs	Plain	Abs	Plain	Abs	Plain	Abs	Plain	Abs	Plain	Abs	Plain	Abs	Plain	Abs	Plain	Abs	Plain	Abs	Plain	Abs	Plain	Abs	Plain	Abs	Plain	Abs	Plain	Abs	Plain	Abs	Plain	Abs	Plain	Abs	Plain	Abs	Plain	Abs	Plain	Abs	Plain	Abs	Plain	Abs	Plain	Abs	Plain	Abs	Plain	Abs	Plain	Abs	Plain	Abs	Plain	Abs	Plain	Abs	Plain	Abs	Plain	Abs	Plain	Abs	Plain	Abs	Plain	Abs	Plain	Abs	Plain	Abs	Plain	Abs	Plain	Abs	Plain	Abs	Plain	Abs	Plain	Abs	Plain	Abs	Plain	Abs	Plain	Abs	Plain	Abs	Plain	Abs	Plain	Abs	Plain	Abs	Plain	Abs	Plain	Abs	Plain	Abs	Plain	Abs	Plain	Abs	Plain	Abs	Plain	Abs	Plain	Abs	Plain	Abs	Plain	Abs	Plain	Abs	Plain	Abs	Plain	Abs	Plain	Abs	Plain	Abs	Plain	Abs	Plain	Abs	Plain	Abs	Plain	Abs	Plain	Abs	Plain	Abs	Plain	Abs	Plain	Abs	Plain	Abs	Plain	Abs	Plain	Abs	Plain	Abs	Plain	Abs	Plain	Abs	Plain	Abs	Plain	Abs	Plain	Abs	Plain	Abs	Plain	Abs	Plain	Abs	Plain	Abs	Plain	Abs	Plain	Abs	Plain	Abs	Plain	Abs	Plain	Abs	Plain	Abs	Plain	Abs	Plain	Abs	Plain	Abs	Plain	Abs	Plain	Abs	Plain	Abs	Plain	Abs	Plain	Abs	Plain	Abs	Plain	Abs	Plain	Abs	Plain	Abs	Plain	Abs	Plain	Abs	Plain	Abs	Plain	Abs	Plain	Abs	Plain	Abs	Plain	Abs	Plain	Abs	Plain	Abs	Plain	Abs	Plain	Abs	Plain	Abs	Plain	Abs	Plain	Abs	Plain	Abs	Plain	Abs	Plain	Abs	Plain	Abs	Plain	Abs	Plain	Abs	Plain	Abs	Plain	Abs	Plain	Abs	Plain	Abs	Plain	Abs	Plain	Abs	Plain	Abs	Plain	Abs	Plain	Abs	Plain	Abs	Plain	Abs	Plain	Abs	Plain	Abs	Plain	Abs	Plain	Abs	Plain	Abs	Plain	Abs	Plain	Abs	Plain	Abs	Plain	Abs	Plain	Abs	Plain	Abs	Plain	Abs	Plain	Abs	Plain	Abs	Plain	Abs	Plain	Abs	Plain	Abs	Plain	Abs	Plain	Abs	Plain	Abs	Plain	Abs	Plain	Abs	Plain	Abs	Plain	Abs	Plain	Abs	Plain	Abs	Plain	Abs	Plain	Abs	Plain	Abs	Plain	Abs	Plain	Abs	Plain	Abs	Plain	Abs	Plain	Abs	Plain	Abs	Plain	Abs	Plain	Abs	Plain	Abs	Plain	Abs	Plain	Abs	Plain	Abs	Plain	Abs	Plain	Abs	Plain	Abs	Plain	Abs	Plain	Abs	Plain	Abs	Plain	Abs	Plain	Abs	Plain	Abs	Plain	Abs	Plain	Abs	Plain	Abs	Plain	Abs	Plain	Abs	Plain	Abs	Plain	Abs	Plain	Abs	Plain	Abs	Plain	Abs	Plain	Abs	Plain	Abs	Plain	Abs	Plain	Abs	Plain	Abs	Plain	Abs	Plain	Abs	Plain	Abs	Plain	Abs	Plain	Abs	Plain	Abs	Plain	Abs	Plain	Abs	Plain	Abs	Plain	Abs	Plain	Abs	Plain	Abs	Plain	Abs	Plain	Abs	Plain	Abs	Plain	Abs	Plain	Abs	Plain	Abs	Plain	Abs	Plain	Abs	Plain	Abs	Plain	Abs	Plain	Abs	Plain	Abs	Plain	Abs	Plain	Abs	Plain	Abs	Plain	Abs	Plain	Abs	Plain	Abs	Plain	Abs	Plain	Abs	Plain	Abs	Plain	Abs	Plain	Abs	Plain	Abs	Plain	Abs	Plain	Abs	Plain	Abs	Plain	Abs	Plain	Abs	Plain	Abs	Plain	Abs	Plain	Abs	Plain	Abs	Plain	Abs	Plain	Abs	Plain	Abs	Plain	Abs	Plain	Abs	Plain	Abs	Plain	Abs	Plain	Abs	Plain	Abs	Plain	Abs	Plain	Abs	Plain	Abs	Plain	Abs	Plain	Abs	Plain	Abs	Plain	Abs	Plain	Abs	Plain	Abs	Plain

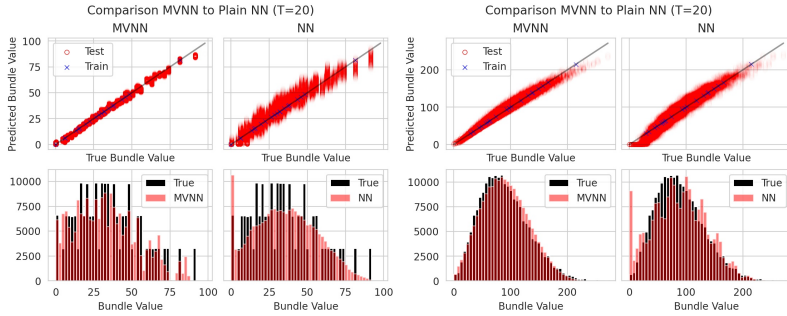
REGIONAL BIDDER

NATIONAL BIDDER

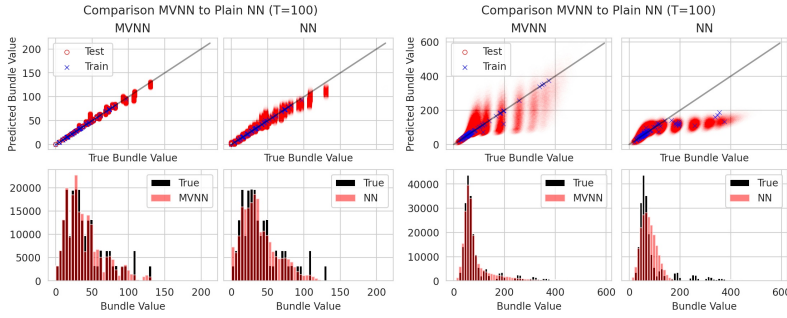
LOCAL BIDDER

HIGH FREQUENCY BIDDER

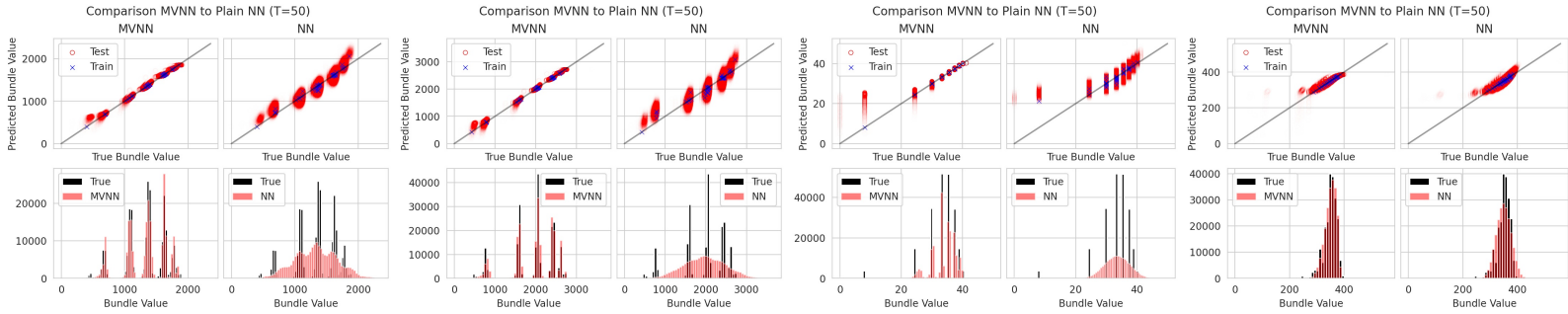
GSVM



LSVM



SRVM



MRVM

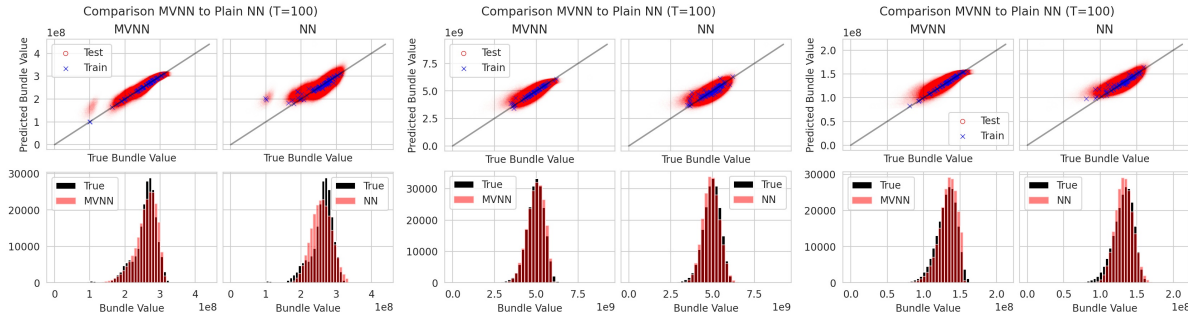


Table 8: Prediction performance comparison for selected MVNNs (MVNN-RELU-PROJECTED) and plain NNs from Table 2 across all domains and bidder types. The top plots compare the quality of the prediction (training data as blue crosses), while the bottom plots focus on how well the models capture the overall value distribution.